

Synthesis and Critical View on the Structure–Activity Relationships of *N*-(Substituted Phenyl)-/*N*-Diphenylmethylpiperazine-Based Conjugates as Antimycobacterial Agents

Jana Čurillová ¹, Mária Pecháčová ¹, Tereza Padrtová ², Daniel Pecher ³, Šárka Mascaretti ⁴, Josef Jampílek ⁵, Ľudmila Pašková ⁶, František Bilka ⁶, Gustáv Kováč ⁷ and Ivan Malík ^{1,*}

¹ Department of Pharmaceutical Chemistry, Faculty of Pharmacy, Comenius University Bratislava, Odbojárov 10, SK-832 32 Bratislava, Slovakia; jana.curillova@uniba.sk; pechacova10@uniba.sk

² Department of Chemical Drugs, Faculty of Pharmacy, Masaryk University, Palackého třída 1946/1, CZ-612 00 Brno, Czech Republic; padrtovat@pharm.muni.cz

³ Department of Pharmaceutical Analysis and Nuclear Pharmacy, Faculty of Pharmacy, Comenius University Bratislava, Odbojárov 10, SK-832 32 Bratislava, Slovakia; pecher1@uniba.sk

⁴ Czech Advanced Technology and Research Institute, Palacky University, Slechtitelu 27, CZ-783 71 Olomouc, Czech Republic; sarka.mascaretti@gmail.com

⁵ Department of Chemical Biology, Faculty of Science, Palacky University, Slechtitelu 27, CZ-783 71 Olomouc, Czech Republic; josef.jampilek@gmail.com

⁶ Department of Cell and Molecular Biology of Drugs, Faculty of Pharmacy, Comenius University Bratislava, Odbojárov 10, SK-832 32 Bratislava, Slovakia; paskova@fpharm.uniba.sk; bilka@fpharm.uniba.sk

⁷ Institute of Chemistry, Clinical Biochemistry and Laboratory Medicine, Faculty of Medicine, Slovak Medical University in Bratislava, Limbová 12, SK-833 03 Bratislava, Slovakia; gustav.kovac@gmail.com

* Correspondence: malik2@uniba.sk (I.M.); Tel.: +421-2-50 117 227

CONTENT

A. Materials and Methods – The Details

A1. The Extension of a Section 2.1. Chemistry in Main Article

The Extension of a Section 2.1.1. General Information in Main Article

The Extension of a Section 2.1.2 Synthesis of Compounds in Main Article

The Extension of a Section 2.1.3 Determination of Some Physicochemical Properties in Main Article

A2. The Extension of a Section 2.2. Biological Assays in Main Article

The Extension of a Section 2.2.1 In Vitro Antimycobacterial Evaluation in Main Article

The Extension of a Section 2.2.2 In Vitro Cytotoxicity Screening in Main Article

A3. The Extension of a Section 2.3 In Silico Evaluation of Synthesized Bases in Main Article

A4. The Extension of a Section 2.4 Calculations and Statistical Analyses in Main Article

A5. The Extension of a Section 3.3. In Silico Evaluation of Synthesized Bases in Main Article

A6. The Extension of a Section 3.4. Structure–Activity Relationships in Main Article

B. Tables

Table S1. Retention times t_r and lipophilicity indices $\log k$ (RP-HPLC) of **6a–g** determined in the mobile phases with a various volume ratio (v/v) of a methanol (MeOH) organic modifier and water, i.e., from 60:40 to 70:30.

Table S2. Retention times t_r and lipophilicity indices $\log k$ (RP-HPLC) of **6a–g** determined in the mobile phases with a various volume ratio (v/v) of a methanol (MeOH) organic modifier and water, i.e., from 75:25 to 90:10.

Table S3. The prediction of probability for the bases (**5a–g**) to act as general pump inhibitors (I_{GPI}) and membrane permeability inhibitors (I_{MPI}) as well as drugs for the treatment of cancer-associated diseases (I_{CADT}). The calculation of probability that these molecules might cause bradycardia (I_B), palpitation (I_P), tachycardia (I_T), and prolongation of a QT interval (I_{QTp}).

Table S4. The selectivity index (SI) values of in vitro evaluated compounds **6a–g**, which were calculated as $SI = IC_{50}$ (in μM units)/MIC (in μM units). The IC_{50} s indicated toxicity in human liver hepatocellular carcinoma (HepG2) cells, the MICs were determined against *M. tuberculosis* H37Ra ATCC 25177 (*Mtb* H37Ra), *M. kansasii* DSM 44162 (MK DSM), *M. smegmatis* ATCC 700084 (MS), and *M. marinum* CAMP 5644 (MM).

Table S5. The contribution of evaluated variables (in percentages) to particular principal components (PCs; PC 1–6).

C. Figures – NMR and HPLC-UV/HR-MS Spectra of Final Compounds

C1. 1H NMR, ^{13}C NMR, ^{19}F NMR and HPLC-UV/HR-MS (ESI) Spectra of 1-[2-Hydroxypropyl-[(3-trifluoromethyl)phenyl]carbamoxyloxy]-4-phenylpiperazin-1-ium Chloride (**6a**)

C2. 1H NMR, ^{13}C NMR, ^{19}F NMR and HPLC-UV/HR-MS (ESI) Spectra of 1-[2-Hydroxypropyl-[(3-trifluoromethyl)phenyl]carbamoxyloxy]-4-(4-methylphenyl)-piperazin-1-ium Chloride (**6b**)

C3. 1H NMR, ^{13}C NMR, ^{19}F NMR and HPLC-UV/HR-MS (ESI) Spectra of 1-[2-Hydroxypropyl-[(3-trifluoromethyl)phenyl]carbamoxyloxy]-4-(4-fluorophenyl)-piperazin-1-ium Chloride (**6c**)

C4. 1H NMR, ^{13}C NMR, ^{19}F NMR and HPLC-UV/HR-MS (ESI) Spectra of 1-[2-Hydroxypropyl-[(3-trifluoromethyl)phenyl]carbamoxyloxy]-4-(4-chlorophenyl)-piperazin-1-ium Chloride (**6d**)

C5. 1H NMR, ^{13}C NMR, ^{19}F NMR and HPLC-UV/HR-MS (ESI) Spectra of 1-[2-Hydroxypropyl-[(3-trifluoromethyl)phenyl]carbamoxyloxy]-4-(3,4-dichlorophenyl)-piperazin-1-ium Chloride (**6e**)

C6. 1H NMR, ^{13}C NMR, ^{19}F NMR and HPLC-UV/HR-MS (ESI) Spectra of 1-[2-Hydroxypropyl-[(3-trifluoromethyl)phenyl]carbamoxyloxy]-4-(3-trifluoromethyl-phenyl)piperazin-1-ium Chloride (**6f**)

C7. 1H NMR, ^{13}C NMR, ^{19}F NMR and HPLC-UV/HR-MS (ESI) Spectra of 1-[2-Hydroxypropyl-[(3-trifluoromethyl)phenyl]carbamoxyloxy]-4-(4-diphenylmethyl)-piperazin-1-ium Chloride (**6g**)

A. Materials and Methods – The Details

All references, which can be found in Supplementary Material, are listed precisely in Main Article. The references are numbered identically in Supplementary Material as in Main Article.

A1. The Extension of a Section 2.1. Chemistry in Main Article

The Extension of a Section 2.1.1. General Information in Main Article

• Yield, Melting Points and TLC Evaluation of All Prepared Compounds – The Details

Yields were given in percentages and referred to the amount of pure products after all purification procedures. Melting point (Mp) values of prepared solid intermediate (**3**) as well as final compounds (**6a–g**) were determined using an open capillary method on a Stuart SMP30 melting point apparatus (Bibby Scientific Limited, Staffordshire, UK) and left uncorrected [30].

The R_f values of all synthesized compounds were obtained by TLC as described in [30]. Petroleum ether/acetone (3:2, *v/v*) eluent was used for the TLC-investigation of the compound **3** and petroleum ether/diethyl amine (8:3, *v/v*) mobile phase was used for TLC of both bases (**5a–g**) and target salts (**6a–g**). Spots were visualized by UV light at a wavelength (λ) of 254 nm.

• Spectral Characterization of All Prepared Compounds – The Details

a) The Infrared (IR) Spectral Characterization

The IR spectra of synthesized intermediates (**3**, **5a–g**) as well as final molecules (**6a–g**) were recorded on a Perkin-Elmer UATR Two spectrometer (Perkin-Elmer Ltd., Beaconsfield, UK) by the technique based on potassium bromide plates. The absorption frequencies ($\tilde{\nu}_{\max}$) were reported in reciprocal centimeters (cm^{-1}) in a recorded range from 4000 cm^{-1} to 400 cm^{-1} . The recorded IR spectra were analyzed with the Perkin-Elmer Spectrum software, *ver.* 10.4.00 (Perkin-Elmer).

Regarding the IR spectra assignment, these abbreviations were used: ν (stretching vibrations), ν_{as} (asymmetric stretching vibrations), ν_{s} (symmetric stretching vibrations), δ (deformation vibrations), δ_{ip} (in-plane deformation vibrations) and δ_{oop} (out-of-plane deformation vibrations), respectively.

b) The Nuclear Magnetic Resonance (NMR) Spectral Characterization

The NMR spectral analyses (^1H NMR, ^{13}C NMR and ^{19}F NMR) were carried out on a JNM-ECZ400R FT-NMR spectrometer 9.39 T (Jeol Resonance, Tokyo, Japan) equipped with a 5 mm High Sensitivity PulseField Gradient Autotune™ probe (Jeol Resonance), operating at 400.0 MHz (^1H NMR), 101.0 MHz (^{13}C NMR) and 376.0 MHz (^{19}F NMR), respectively. The details connected with spectra measurements of synthesized compounds were published [30].

The spectra were measured at 30 °C in dried $\text{DMSO-}d_6$, chemical shifts were reported on a δ scale in parts *per* million (ppm), referenced to chemical shifts of residual solvent resonance ($\text{DMSO-}d_6$; 2.5 ppm for ^1H NMR and 39.5 ppm for ^{13}C NMR, respectively). Coupling constants (J) were given in Hertz (Hz) and spin multiplicities were expressed by abbreviations as follows: s (singlet), bs (broadened singlet), d (doublet), dd (double doublet), q (quartet), m (multiplet). The complete assignment of ^1H NMR, ^{13}C NMR, and ^{19}F NMR resonances was based on the interpretation of standard NMR values.

c) The High-Performance Liquid Chromatography-High-Resolution Mass Spectra (HPLC-UV/HR-MS) Characterization

The HPLC-UV/HR-MS analyses of all prepared compounds were carried out on an HPLC Agilent Infinity System (Agilent Technologies, Santa Clara, CA, USA) equipped with a gradient pump (1260 Binary Pump VL; Agilent Technologies), automatic injector (1260 HiPals; Agilent Technologies), and column thermostat (1290 TCC; Agilent Technologies). The HPLC system was coupled with a quadrupole time-of-flight mass spectrometer (6520 Accurate-Mass Q-TOF LC/MS; Agilent Technologies) equipped with an electrospray ionization source operated in a positive ionization mode.

All analyzed compounds were dissolved in dimethyl sulfoxide (DMSO) for HPLC (Merck, Darmstadt, Germany); volume 1.0 μ L was used for each HPLC-UV/HR-MS analysis. The specifications and conditions for MS measurements as well as procedures to estimate lipophilicity descriptors were published [30].

Personal computer with the MassHunter Workstation software, ver. B.05.01 (Agilent Technologies) was used for acquisition and processing of data from the HPLC-UV/HR-MS apparatus [30].

d) The Ultraviolet/Visible (UV/Vis) Spectral Characterization

The UV/Vis spectra of methanolic solutions of final compounds **6a–g** ($c = 5.0 \times 10^{-5}$ M) were observed on a Diode Array HP-8452A Spectrophotometer (Hewlett-Packard, Palo Alto, CA, USA) at 21 °C. Methanol for UV-spectroscopy (Merck, Darmstadt, Germany) was used for the preparation of these solutions. Results of the UV/Vis analyses were collected and stored digitally using the ChemStation controller software (Agilent Technologies, Waldbronn, Germany). The HP-8452A apparatus measured a complete range of compounds' spectrum from 190 nm to 820 nm, as listed in [31].

The Extension of a Section 2.1.2 Synthesis of Compounds in Main Article

• Preparation of (\pm)-(Oxiran-2-yl)methyl-[1-(3-Trifluoromethyl)phenyl]carbamate (**3**) – The Details

a) Synthesis

Into a stirred solution of 3-(trifluoromethyl)phenyl isocyanate **1** (CAS Registry Number 329-01-1; 6.00 g, 32 mmol) in 80 mL of anhydrous toluene, a solution of (\pm)-(oxiran-2-yl)methanol **2** (CAS Registry Number 556-52-5; 2.60 g, 35 mmol) in 10 mL of anhydrous toluene was added dropwise. The mixture was stirred continuously at 70 °C for 25 h. When the reaction was completed (TLC control), the solvent was evaporated *in vacuo*, crude intermediate **3** was dissolved in chloroform and washed with 3×100 mL of distilled water. The organic layer was collected, dried properly over anhydrous magnesium sulfate, and evaporated *in vacuo* to give a crude solid product **3**, which was crystallized from cyclohexane.

b) Spectral Characterization of The Compound **3**

The parameters characterizing given off-white solid (Figure 4 in Main Article), i.e., yield, M_r , M_p , R_f , ^1H NMR, ^{13}C NMR, ^{19}F NMR, HPLC-UV/HR-MS (ESI), were available [30]. Thus, some missing data, i.e., IR spectra and purity, were estimated in current research. The complete characterization of **3** is provided below.

(\pm)-(Oxiran-2-yl)methyl-[1-(3-trifluoromethyl)phenyl]carbamate (**3**). Yield 6.77 g (81%); M_r 261.20; R_f 0.64 (petroleum ether/acetone 3:2); M_p 138–139 °C; IR (UATR): 3285 (ν NH), 2955 (ν_{as} CH₂), 2820 (ν_s CH₂), 1726 (ν C=O), 1605 (ν C=C), 1510 (δ NH), 1492 (ν CN), 1245 (ν_{as} C–O–C), 1064 (ν_s C–O), 1022 (δ_{ip} =C–H), 848 (δ_{oop} =C–H) cm^{-1} ; ^1H NMR (400.0 MHz, DMSO- d_6) δ_H (ppm): 10.14 (s, 1H, NHCOO), 7.90 (s, 1H, Ar–H), 7.70–7.68 (m, 1H, Ar–H), 7.54–7.50 (m, 1H, Ar–H), 7.35–7.33 (m, 1H, Ar–H), 4.50 (dd, 1H, $^1J = 12.3$ Hz, $^2J = 2.7$ Hz, OCH₂CH), 3.90 (dd, 1H, $^1J = 12.3$ Hz, $^2J = 6.6$ Hz, OCH₂CH), 3.29–3.24 (m, 1H, CH oxiran-2-yl), 2.83–2.81 (m, 1H, CH₂ oxiran-2-yl), 2.69 (dd, 1H, $^1J = 5.1$ Hz, $^2J = 2.6$ Hz, CH₂ oxiran-2-yl); ^{13}C NMR (101.0 MHz, DMSO- d_6) δ (ppm): 153.2, 139.8, 130.0, 130.0–129.1 (q, $^2J = 31.5$ Hz), 128.1–120.0 (q, $^1J = 272.2$ Hz), 121.8, 118.8, 114.1, 65.4, 49.1, 43.8; ^{19}F NMR (376.0 MHz, DMSO- d_6) δ_F (ppm): -60.20 (s, Ar–CF₃); HPLC-UV/HR-MS (ESI): for C₁₁H₁₀O₃F₃N [M+H]⁺ calculated 262.0686 m/z , found 262.0681 m/z , Difference (ppm) 1.17; Purity (LC-UV/HR-MS): 98.99%.

• Preparation of 3-[4-(4-Chloro)phenyl]-4-(3,4-Dichloro)phenyl-4-(Diphenylmethyl)-/-4-(4-Fluoro)phenyl-4-(4-Methyl)phenyl-/Phenyl-4-(3-Trifluoromethyl)phenylpiperazin-1-yl]-/-2-Hydroxypropyl-1-[(3-Trifluoromethyl)phenyl]carbamates (**5a–g**) – The Details

a) Synthesis

Into a stirred solution of an oxirane moiety-containing compound **3** (3.10 g, 12 mmol) in 40 mL of anhydrous propan-2-ol, a solution of 1-phenylpiperazine **4a** (CAS Registry Number 92-54-6; 1.95 g, 12 mmol), 1-(4-methylphenyl)piperazine **4b** (CAS Registry Number 39593-08-3; 2.12 g, 12 mmol), 1-(4-fluorophenyl)piperazine **4c** (CAS Registry Number 2252-63-3; 2.16 g, 12 mmol), 1-(4-chlorophenyl)piperazine **4d** (CAS

Registry Number 38212-33-8; 2.36 g, 12 mmol), 1-(3,4-dichlorophenyl)piperazine **4e** (CAS Registry Number 57260-67-0; 2.77 g, 12 mmol), 1-(3-trifluoromethylphenyl)piperazine **4f** (CAS Registry Number 15532-75-9; 2.76 g, 12 mmol) or 1-(diphenylmethyl)piperazine **4g** (CAS Registry Number 841-77-0; 3.01 g, 12 mmol) in 30 mL of anhydrous propan-2-ol was added dropwise.

Each mixture was stirred continuously at reflux for 20 h. When the reaction was completed (TLC control), the solvent was evaporated *in vacuo*, crude molecules **5a–d** were dissolved in chloroform and washed with 3 × 100 mL of distilled water. The organic layer was collected, dried properly over anhydrous magnesium sulfate, and evaporated *in vacuo*, providing viscous (oily) yellowish products **5a–g** (Figure 4 in Main Article).

b) Spectral Characterization of The Compounds **5a–g**

The R_f values of **5a–g** were estimated in a petroleum ether/diethyl amine (8:3, *v/v*) mobile phase.

2-Hydroxypropyl-3-(4-phenylpiperazin-1-yl)-1-[(3-trifluoromethyl)phenyl]carbamate (5a). Yield 3.53 g (78%); M_r 423.43; R_f 0.45; IR (UATR): 3560 (ν OH), 3322 (ν NH), 2961 (ν_{as} CH₂), 2880 (ν_s CH₂), 1725 (ν C=O), 1605 (ν C=C), 1510 (δ NH), 1499 (ν CN), 1244 (ν_{as} C–O–C), 1064 (ν_s C–O), 1022 (δ_{ip} =C–H), 848 (δ_{oop} =C–H) cm⁻¹; ¹H NMR (400.0 MHz, DMSO-*d*₆) δ_H (ppm): 10.02 (s, 1H, NHCOO), 7.92 (s, 1H, Ar–H), 7.70 (d, J = 8.4 Hz, 1H, Ar–H), 7.52–7.49 (m, 1H, Ar–H), 7.33 (d, 1H, J = 6.9 Hz, Ar–H), 7.22–7.18 (m, 2H, Ar–H), 6.92–6.90 (m, 2H, Ar–H), 6.78–6.74 (m, 1H, Ar–H), 4.85 (bs, 1H, OH), 4.22 (dd, 1J = 10.9 Hz, 2J = 3.8 Hz, 1H, OCH₂), 4.02 (dd, 1J = 10.9 Hz, 2J = 6.5 Hz, 1H, OCH₂), 3.94 (m, 1H, CHOH), 3.13–3.10 (m, 4H, CH₂N piperazine), 2.64–2.40 (overlap, m, 6H, CH₂N, CH₂N piperazine); ¹³C NMR (101.0 MHz, DMSO-*d*₆) δ_C (ppm): 153.6, 151.0, 140.1, 129.9, 129.6–128.9 (q, 2J = 31.5 Hz), 128.1–119.8 (1J = 272.2 Hz), 122.1, 121.7, 118.7, 115.2, 114.0, 67.5, 66.0, 61.0, 53.4, 48.2; ¹⁹F NMR (376.0 MHz, DMSO-*d*₆) δ_F (ppm): -60.12 (s, Ar–CF₃); HPLC-UV/HR-MS (ESI): for C₂₁H₂₄O₃F₃N₃ [M+H]⁺ calculated 424.1843 *m/z*, found 424.1848 *m/z*, Difference (ppm) -1.18; Purity (LC-UV/HR-MS): 97.53%.

2-Hydroxypropyl-3-[4-(4-methylphenyl)piperazin-1-yl]-1-[(3-trifluoromethyl)phenyl]carbamate (5b). Yield 3.47 g (79%); M_r 437.46; R_f 0.49; IR (UATR): 3562 (ν OH), 3322 (ν NH), 2959 (ν_{as} CH₂), 2879 (ν_s CH₂), 1724 (ν C=O), 1606 (ν C=C), 1512 (δ NH), 1495 (ν CN), 1245 (ν_{as} C–O–C), 1062 (ν_s C–O), 1020 (δ_{ip} =C–H), 848 (δ_{oop} =C–H) cm⁻¹; ¹H NMR (400.0 MHz, DMSO-*d*₆) δ_H (ppm): 10.02 (s, 1H, NHCOO), 7.92 (s, 1H, Ar–H), 7.70 (d, J = 8.3 Hz, 1H, Ar–H), 7.53–7.49 (m, 1H, Ar–H), 7.32 (d, J = 8.5 Hz, 1H, Ar–H), 7.01–6.99 (m, 2H, Ar–H), 6.81–6.79 (m, 2H, Ar–H), 4.85–4.84 (bs, 1H, OH), 4.21 (dd, 1J = 11.0 Hz, 2J = 3.8 Hz, 1H, OCH₂), 4.02 (dd, 1J = 11.0 Hz, 2J = 6.5 Hz, 1H, OCH₂), 3.93 (m, 1H, CHOH), 3.06–3.04 (m, 4H, CH₂N piperazine), 2.63–2.37 (overlap, m, 6H, CH₂N, CH₂N piperazine), 2.19 (s, 3H, Ar–CH₃); ¹³C NMR (101.0 MHz, DMSO-*d*₆) δ_C (ppm): 153.6, 148.9, 140.1, 130.0–129.0 (q, J = 31.8 Hz), 129.9, 128.1–120.0 (q, J = 272.6 Hz), 127.5, 121.7, 118.5, 115.5, 114.0, 53.4, 48.7, 19.9; ¹⁹F NMR (376.0 MHz, DMSO-*d*₆) δ_F (ppm): -60.19 (s, Ar–CF₃); HPLC-UV/HR-MS (ESI): for C₂₂H₂₆O₃F₃N₃ [M+H]⁺ calculated 438.1999 *m/z*, found 438.2001 *m/z*, Difference (ppm) -1.46; Purity (LC-UV/HR-MS): 98.72%.

3-[4-(4-Fluorophenyl)piperazin-1-yl]-2-hydroxypropyl-1-[(3-trifluoromethyl)phenyl]carbamate (5c). Yield 3.35 g (79%); M_r 441.42; R_f 0.50; IR (UATR): 3559 (ν OH), 3320 (ν NH), 2959 (ν_{as} CH₂), 2892 (ν_s CH₂), 1733 (ν C=O), 1605 (ν C=C), 1510 (δ NH), 1495 (ν CN), 1244 (ν_{as} C–O–C), 1154 (ν CF), 1062 (ν_s C–O), 1020 (δ_{ip} =C–H), 845 (δ_{oop} =C–H) cm⁻¹; ¹H NMR (400.0 MHz, DMSO-*d*₆) δ_H (ppm): 10.10 (s, 1H, NHCOO), 7.68 (d, J = 13.07 Hz, 2H, Ar–H), 7.20–7.12 (m, 6H, Ar–H), 4.14 (bs, 1H, OH), 4.09 (dd, 1J = 11.0 Hz, 2J = 3.8 Hz, 1H, OCH₂), 4.02 (dd, 1J = 11.0 Hz, 2J = 6.5 Hz, 1H, OCH₂), 3.91 (m, 1H, CHOH), 3.08–3.04 (m, 4H, CH₂N piperazine), 2.63–2.37 (overlap, m, 6H, CH₂N, CH₂N piperazine); ¹³C NMR (101.0 MHz, DMSO-*d*₆) δ_C (ppm): 154.7, 145.9, 142.2, 130.6, 125.1, 118.5, 117.1, 65.2, 61.2, 55.5, 53.9, 51.8, 46.7, 46.7, 46.3, 28.9; ¹⁹F NMR (376.0 MHz, DMSO-*d*₆) δ_F (ppm): -60.23 (s, Ar–CF₃), -125.19 (s, Ar–F); HPLC-UV/HR-MS (ESI): for C₂₁H₂₃O₃F₄N₃ [M+H]⁺ calculated 442.1748 *m/z*, found 442.1766 *m/z*, Difference (ppm) -4.07; Purity (LC-UV/HR-MS): 98.63%.

3-[4-(4-Chlorophenyl)piperazin-1-yl]-2-hydroxypropyl-1-[(3-trifluoromethyl)phenyl]carbamate (5d). Yield 3.82 g (84%); M_r 457.87; R_f 0.55; IR (UATR): 3566 (ν OH), 3320 (ν NH),

2955 ($\nu_{\text{as}} \text{CH}_2$), 2885 ($\nu_{\text{s}} \text{CH}_2$), 1729 ($\nu \text{C=O}$), 1606 ($\nu \text{C=C}$), 1510 (δNH), 1495 (νCN), 1245 ($\nu_{\text{as}} \text{C-O-C}$), 1150 (νCF), 1062 ($\nu_{\text{s}} \text{C-O}$), 1020 ($\delta_{\text{ip}} =\text{C-H}$), 848 ($\delta_{\text{oop}} =\text{C-H}$), 740 ($\gamma \text{C-Cl}$) cm^{-1} ; ^1H NMR (400.0 MHz, $\text{DMSO-}d_6$) δ_{H} (ppm): 10.25 (s, 1H, NHCOO), 7.94 (s, 1H, Ar-H), 7.72 (d, $J = 8.8 \text{ Hz}$, 1H, Ar-H), 7.54–7.50 (m, 1H, Ar-H), 7.45–7.43 (m, 1H, Ar-H), 7.33 (d, $J = 7.8 \text{ Hz}$, 1H, Ar-H), 7.24–7.23 (m, 1H, Ar-H), 7.01–6.98 (m, 1H, Ar-H), 6.39 (bs, 1H, Ar-H), 4.11 (bs, 1H, OH), 4.07 (dd, $^1J = 11.0 \text{ Hz}$, $^2J = 3.8 \text{ Hz}$, 1H, OCH_2), 4.01 (dd, $^1J = 11.0 \text{ Hz}$, $^2J = 6.5 \text{ Hz}$, 1H, OCH_2), 3.88 (m, 1H, CHOH), 3.10–3.05 (m, 4H, CH_2N piperazine), 2.65–2.34 (overlap, m, 6H, $\text{CH}_2\text{N}, \text{CH}_2\text{N}$ piperazine); ^{13}C NMR (101.0 MHz, $\text{DMSO-}d_6$) δ_{C} (ppm): 153.3, 149.3, 140.0, 131.7, 130.7, 130.0, 130.0–129.0 (q, $J = 31.6 \text{ Hz}$), 128.2–120.1 (q, $J = 272.1 \text{ Hz}$), 121.8, 120.8, 118.8, 116.9, 115.8, 114.1, 66.2, 63.5, 58.3, 51.8, 50.6, 44.6, 42.1; ^{19}F NMR (376.0 MHz, $\text{DMSO-}d_6$) δ_{F} (ppm): -60.00 (s, Ar- CF_3); HPLC-UV/HR-MS (ESI): for $\text{C}_{21}\text{H}_{23}\text{O}_3\text{ClF}_3\text{N}_3$ $[\text{M}+\text{H}]^+$ calculated 458.1453 m/z , found 458.1465 m/z , Difference (ppm) -2.62; Purity (LC-UV/HR-MS): 97.99%.

3-[4-(3,4-Dichlorophenyl)piperazin-1-yl]-2-hydroxypropyl-1-[(3-trifluoromethyl)phenyl]-carbamate (**5e**). Yield 4.03 g (82%); M_r 491.10; R_f 0.60; IR (UATR): 3567 (νOH), 3318 (νNH), 2935 ($\nu_{\text{as}} \text{CH}_2$), 2879 ($\nu_{\text{s}} \text{CH}_2$), 1731 ($\nu \text{C=O}$), 1605 ($\nu \text{C=C}$), 1512 (δNH), 1496 (νCN), 1242 ($\nu_{\text{as}} \text{C-O-C}$), 1150 (νCF), 1063 ($\nu_{\text{s}} \text{C-O}$), 1020 ($\delta_{\text{ip}} =\text{C-H}$), 845 ($\delta_{\text{oop}} =\text{C-H}$), 735 ($\gamma \text{C-Cl}$) cm^{-1} ; ^1H NMR (400.0 MHz, $\text{DMSO-}d_6$) δ_{H} (ppm): 10.15 (s, 1H, NHCOO), 7.83 (s, 1H, Ar-H), 7.75 (d, $J = 8.9 \text{ Hz}$, 1H, Ar-H), 7.54–7.50 (m, 1H, Ar-H), 7.48–7.44 (m, 1H, Ar-H), 7.34 (d, 1H, $J = 7.8 \text{ Hz}$, Ar-H), 7.29 (d, 1H, $J = 8.6 \text{ Hz}$, Ar-H), 7.27 (s, 1H, Ar-H), 7.14 (d, $J = 7.5 \text{ Hz}$, 1H, Ar-H), 4.25 (bs, 1H, OH), 4.04 (dd, $^1J = 11.0 \text{ Hz}$, $^2J = 3.8 \text{ Hz}$, 1H, OCH_2), 4.01 (dd, $^1J = 11.0 \text{ Hz}$, $^2J = 6.5 \text{ Hz}$, 1H, OCH_2), 3.96 (m, 1H, CHOH), 3.12–3.05 (m, 4H, CH_2N piperazine), 2.66–2.37 (overlap, m, 6H, $\text{CH}_2\text{N}, \text{CH}_2\text{N}$ piperazine); ^{13}C NMR (101.0 MHz, $\text{DMSO-}d_6$) δ_{C} (ppm): 155.4, 147.8, 139.2, 130.3, 130.2, 130.0–129.1 (q, $^2J = 32.6 \text{ Hz}$), 129.9, 129.6, 128.4–120.3 (q, $^1J = 272.8 \text{ Hz}$), 128.2–120.1 (q, $J = 272.1 \text{ Hz}$), 121.8, 119.2, 114.1, 111.6, 66.2, 63.5, 58.3, 52.0, 50.8, 44.7, 44.6, 42.3; ^{19}F NMR (376.0 MHz, $\text{DMSO-}d_6$) δ_{F} (ppm): -60.32 (s, Ar- CF_3); HPLC-UV/HR-MS (ESI): for $\text{C}_{21}\text{H}_{22}\text{O}_3\text{Cl}_2\text{F}_3\text{N}_3$ $[\text{M}+\text{H}]^+$ calculated 492.1063 m/z , found 492.1078 m/z , Difference (ppm) -3.05; Purity (LC-UV/HR-MS): 97.62%.

2-Hydroxypropyl-3-[4-(3-trifluoromethylphenyl)piperazin-1-yl]-1-[(3-trifluoromethyl)phenyl]carbamate (**5f**). Yield 3.47 g (79%); M_r 491.43; R_f 0.59; IR (UATR): 3571 (νOH), 3317 (νNH), 2963 ($\nu_{\text{as}} \text{CH}_2$), 2857 ($\nu_{\text{s}} \text{CH}_2$), 1740 ($\nu \text{C=O}$), 1606 ($\nu \text{C=C}$), 1512 (δNH), 1495 (νCN), 1245 ($\nu_{\text{as}} \text{C-O-C}$), 1152 (νCF), 1063 ($\nu_{\text{s}} \text{C-O}$), 1020 ($\delta_{\text{ip}} =\text{C-H}$), 845 ($\delta_{\text{oop}} =\text{C-H}$) cm^{-1} ; ^1H NMR (400.0 MHz, $\text{DMSO-}d_6$) δ_{H} (ppm): 10.07 (s, 1H, NHCOO), 7.92 (s, 1H, Ar-H), 7.71–7.69 (m, 1H, Ar-H), 7.53–7.49 (m, 1H, Ar-H), 7.42–7.38 (m, 1H, Ar-H), 7.33–7.31 (m, 1H, Ar-H), 7.21–7.19 (m, 1H, Ar-H), 7.06–7.04 (m, 1H, Ar-H), 4.88 (bs, 1H, OH), 4.11 (dd, $^1J = 11.0 \text{ Hz}$, $^2J = 3.8 \text{ Hz}$, 1H, OCH_2), 4.07 (dd, $^1J = 11.0 \text{ Hz}$, $^2J = 6.5 \text{ Hz}$, 1H, OCH_2), 3.87 (m, 1H, CHOH), 3.17–3.09 (m, 4H, CH_2N piperazine), 2.61–2.35 (overlap, m, 6H, $\text{CH}_2\text{N}, \text{CH}_2\text{N}$ piperazine); ^{13}C NMR (101.0 MHz, $\text{DMSO-}d_6$) δ_{C} (ppm): 160.9, 153.7, 151.2, 140.2, 130.1–129.7 (m), 125.8–118.7 (m, $^1J = 272.1 \text{ Hz}$), 121.7, 115.2, 114.5, 114.0, 111.8, 110.8, 67.6, 66.1, 61.0, 53.2, 48.7, 47.6, 44.4; ^{19}F NMR (376.0 MHz, $\text{DMSO-}d_6$) δ_{F} (ppm): -60.22 (s, Ar- CF_3), -60.49 (Ar- CF_3); HPLC-UV/HR-MS (ESI): for $\text{C}_{22}\text{H}_{23}\text{O}_3\text{F}_6\text{N}_3$ $[\text{M}+\text{H}]^+$ calculated 492.1716 m/z , found 492.1708 m/z , Difference (ppm) 1.63; Purity (LC-UV/HR-MS): 98.96%.

3-[4-(3,4-Diphenylmethyl)piperazin-1-yl]-2-hydroxypropyl-1-[(3-trifluoromethyl)phenyl]-carbamate (**5g**). Yield 4.33 g (84%); M_r 513.55; R_f 0.63; IR (UATR): 3568 (νOH), 3322 (νNH), 2959 ($\nu_{\text{as}} \text{CH}_2$), 2871 ($\nu_{\text{s}} \text{CH}_2$), 1738 ($\nu \text{C=O}$), 1606 ($\nu \text{C=C}$), 1512 (δNH), 1495 (νCN), 1243 ($\nu_{\text{as}} \text{C-O-C}$), 1151 (νCF), 1062 ($\nu_{\text{s}} \text{C-O}$), 1020 ($\delta_{\text{ip}} =\text{C-H}$), 845 ($\delta_{\text{oop}} =\text{C-H}$) cm^{-1} ; ^1H NMR (400.0 MHz, $\text{DMSO-}d_6$) δ_{H} (ppm): 9.99 (s, 1H, NHCOO), 7.90 (s, 1H, Ar-H), 7.69–7.68 (m, 1H, Ar-H), 7.52–7.49 (m, 1H, Ar-H), 7.41–7.15 (overlap, m, 11H, Ar-H), 4.76 (bs, 1H, OH), 4.09 (dd, $^1J = 11.0 \text{ Hz}$, $^2J = 3.8 \text{ Hz}$, 1H, OCH_2), 4.07 (dd, $^1J = 11.0 \text{ Hz}$, $^2J = 6.5 \text{ Hz}$, 1H, OCH_2), 3.86 (m, 1H, CHOH), 3.08–3.02 (m, 4H, CH_2N piperazine), 2.58–2.31 (overlap, m, 6H, $\text{CH}_2\text{N}, \text{CH}_2\text{N}$ piperazine); ^{13}C NMR (101.0 MHz, $\text{DMSO-}d_6$) δ_{C} (ppm): 153.6, 142.8, 140.1, 129.9, 129.6, 129.3, 128.4, 127.5, 126.7, 121.7, 118.5, 114.0, 75.1, 67.5, 65.8, 61.0, 53.5, 51.5; ^{19}F NMR (376.0 MHz, $\text{DMSO-}d_6$) δ_{F} (ppm): -60.23 (s, Ar- CF_3); HPLC-UV/HR-MS (ESI): for $\text{C}_{28}\text{H}_{30}\text{O}_3\text{F}_3\text{N}_3$ $[\text{M}+\text{H}]^+$ calculated 514.2312 m/z , found 514.2327 m/z , Difference (ppm) -2.92; Purity (LC-UV/HR-MS): 99.59%.

• Preparation of 1-[2-Hydroxypropyl]-{(3-Trifluoromethyl)phenyl}carbamoyloxy]-4-
-(4-Chlorophenyl)-/(3,4-Dichlorophenyl)-/(4-Diphenylmethyl)-/(4-Fluorophenyl)-/(4-Methylphenyl)-/Phenyl-/ (3-Trifluoromethyl)piperazin-1-ium Chlorides (**6a–g**) – The Details

a) Synthesis

The solution of a synthesized base, i.e., **5a** (2.54 g, 6 mmol), **5b** (2.63 g, 6 mmol), **5c** (2.65 g, 6 mmol), **5d** (2.75 g, 6 mmol), **5e** (2.95 g, 6 mmol), **5f** (2.95 g, 6 mmol) and **5g** (3.08 g, 6 mmol), respectively, in 60 mL of chloroform was treated with a saturated solution of hydrogen chloride in diethyl ether and stirred for 5 h at laboratory temperature. The solvents were removed *in vacuo*, and solid crude products were crystallized from 2-propanol. The crystallization process was repeated in the attempt to obtain pure molecules.

b) Spectral Characterization of The Compounds **6a–g**

The R_f values of **6a–g** were estimated in a petroleum ether/diethyl amine (8:3, *v/v*) mobile phase.

1-[2-Hydroxypropyl]-{(3-trifluoromethyl)phenyl}carbamoyloxy]-4-phenylpiperazin-1-ium chloride (**6a**). Yield 1.62 g (35%); M_r 459.89; R_f 0.49; Mp 163–165 °C; IR (UATR): 3552 (ν OH), 3334 (ν NH), 2958 (ν_{as} CH₂), 2878 (ν_s CH₂), 1730 (ν C=O), 1605 (ν C=C), 1510 (δ NH), 1499 (ν CN), 1245 (ν_{as} C–O–C), 1064 (ν_s C–O), 1020 (δ_{ip} =C–H), 848 (δ_{oop} =C–H) cm⁻¹; ¹H NMR (400.0 MHz, DMSO-*d*₆) δ_H (ppm): 10.93 (s, 1H, NH⁺), 10.24 (s, 1H, NHCOO), 7.90 (s, 1H, Ar–H), 7.70 (d, J = 8.1 Hz, 1H, Ar–H), 7.50–7.46 (m, 1H, Ar–H), 7.30 (d, 1H, J = 7.6 Hz, Ar–H), 7.29–7.25 (m, 2H, Ar–H), 7.00–6.98 (m, 2H, Ar–H), 6.86–6.84 (m, 1H, Ar–H), 4.85 (bs, 1H, OH), 4.40 (dd, 1J = 11.0 Hz, 2J = 3.8 Hz, 1H, OCH₂), 4.08 (dd, 1J = 11.0 Hz, 2J = 6.5 Hz, 1H, OCH₂), 3.75 (m, 1H, CHOH), 3.25–3.23 (m, 4H, CH₂N piperazine); ¹³C NMR (101.0 MHz, DMSO-*d*₆) δ_C (ppm): 153.8, 149.8, 140.5, 130.5, 130.5–129.8 (q, 2J = 31.8 Hz), 129.8, 126.0, 122.3, 120.9, 119.3, 119.3, 117.2, 116.6, 66.8, 64.1, 58.8, 52.6, 51.5, 46.6, 45.9, 42.7; ¹⁹F NMR (376.0 MHz, DMSO-*d*₆) δ_F (ppm): -60.16 (s, Ar–CF₃); HPLC-UV/HR-MS (ESI): for C₂₁H₂₄O₃F₃N₃ [M+H]⁺ calculated 424.1843 *m/z*, found 424.1850 *m/z*, Difference (ppm) -0.14; Purity (LC-UV/HR-MS): 97.34%.

1-[2-Hydroxypropyl]-{(3-trifluoromethyl)phenyl}carbamoyloxy]-4-(4-methylphenyl)piperazin-1-ium chloride (**6b**). Yield 2.01 g (42%); M_r 473.92; R_f 0.51; Mp 151–152 °C; IR (UATR): 3555 (ν OH), 3324 (ν NH), 2964 (ν_{as} CH₂), 2873 (ν_s CH₂), 1732 (ν C=O), 1606 (ν C=C), 1512 (δ NH), 1495 (ν CN), 1242 (ν_{as} C–O–C), 1062 (ν_s C–O), 1022 (δ_{ip} =C–H), 848 (δ_{oop} =C–H) cm⁻¹; ¹H NMR (400.0 MHz, DMSO-*d*₆) δ_H (ppm): 10.95 (s, 1H, NH⁺), 10.23 (s, 1H, NHCOO), 7.90 (s, 1H, Ar–H), 7.70 (d, J = 8.8 Hz, 1H, Ar–H), 7.50–7.46 (m, 1H, Ar–H), 7.31 (d, J = 7.8 Hz, 1H, Ar–H), 7.29 (bs, 1H, Ar–H), 7.07–7.05 (m, 2H, Ar–H), 6.95–6.93 (m, 1H, Ar–H), 4.40 (bs, 1H, OH), 4.37 (dd, 1J = 11.0 Hz, 2J = 3.8 Hz, 1H, OCH₂), 4.09 (dd, 1J = 11.0 Hz, 2J = 6.5 Hz, 1H, OCH₂), 3.58 (m, 1H, CHOH), 3.36–3.16 (m, 4H, CH₂N piperazine); ¹³C NMR (101.0 MHz, DMSO-*d*₆) δ_C (ppm): 153.8, 147.1, 140.5, 130.5–129.8 (q, 2J = 32.3 Hz), 130.2, 129.8, 129.8, 126.0, 122.3, 119.3, 117.3, 114.3, 66.8, 64.1, 58.8, 52.5, 51.4, 46.7, 20.7; ¹⁹F NMR (376.0 MHz, DMSO-*d*₆) δ_F (ppm): -60.14 (s, Ar–CF₃); HPLC-UV/HR-MS (ESI): for C₂₂H₂₆O₃F₃N₃ [M+H]⁺ calculated 438.1999 *m/z*, found 438.1998 *m/z*, Difference (ppm) -0.06; Purity (LC-UV/HR-MS): 98.72%.

1-[2-Hydroxypropyl]-{(3-trifluoromethyl)phenyl}carbamoyloxy]-4-(4-fluorophenyl)piperazin-1-ium chloride (**6c**). Yield 1.49 g (31%); M_r 477.88; R_f 0.57; Mp 162–163 °C; IR (UATR): 3551 (ν OH), 3395 (ν NH), 2955 (ν_{as} CH₂), 2868 (ν_s CH₂), 1722 (ν C=O), 1605 (ν C=C), 1510 (δ NH), 1490 (ν CN), 1242 (ν_{as} C–O–C), 1152 (ν CF), 1062 (ν_s C–O), 1020 (δ_{ip} =C–H), 845 (δ_{oop} =C–H) cm⁻¹; ¹H NMR (400.0 MHz, DMSO-*d*₆) δ_H (ppm): 10.11 (s, 1H, NH⁺), 9.99 (s, 1H, NHCOO), 7.77–7.58 (m, 4H, Ar–H), 7.22 (dd, J = 8.0, 5.7 Hz, 2H, Ar–H), 6.93 (dd, J = 9.2, 2.7 Hz, 2H, Ar–H), 4.99–4.84 (m, 1H), 4.21 (dd, 1J = 10.9 Hz, 2J = 3.9 Hz, 1H, OCH₂), 4.10–3.95 (m, 1H, OCH₂), 3.14–3.03 (m, 5H, CH₂N piperazine), 2.93–2.87 (m, 1H), 2.57 (dd, 1J = 10.6 Hz, 2J = 5.3 Hz, 3H), 2.46–2.24 (m, 2H); ¹³C NMR (101.0 MHz, DMSO-*d*₆) δ_C (ppm): 153.9, 153.4, 153.4, 150.6, 150.2, 129.03, 126.49, 122.7, 118.3, 118.2, 117.3, 68.4, 68.0, 66.5, 61.4, 53.7, 48.8, 48.5, 45.3; ¹⁹F NMR (376.0 MHz, DMSO-*d*₆) δ_F (ppm): -60.20 (s, Ar–CF₃), -124.23 (s, Ar–F); HPLC-UV/HR-MS (ESI): for C₂₁H₂₃O₃F₄N₃ [M+H]⁺ calculated 442.1748 *m/z*, found 442.1762 *m/z*, Difference (ppm) -3.15; Purity (LC-UV/HR-MS): 98.51%.

1-[2-Hydroxypropyl-((3-trifluoromethyl)phenyl)carbamoyloxy]-4-(4-chlorophenyl)piperazin-1-ium chloride (**6d**). Yield 1.86 g (38%); M_r 494.34; R_f 0.57; M_p 164–165 °C; IR (UATR): 3546 (ν OH), 3392 (ν NH), 2959 (ν_{as} CH₂), 2869 (ν_s CH₂), 1725 (ν C=O), 1606 (ν C=C), 1510 (δ NH), 1495 (ν CN), 1242 (ν_{as} C–O–C), 1152 (ν CF), 1064 (ν_s C–O), 1020 (δ_{ip} =C–H), 846 (δ_{oop} =C–H), 740 (γ C–Cl) cm⁻¹; ¹H NMR (400.0 MHz, DMSO-*d*₆) δ_H (ppm): 10.91 (s, 1H, NH⁺), 10.22 (s, 1H, NHCOO), 7.89 (s, 1H, Ar–H), 7.68 (d, J = 8.5 Hz, 1H, Ar–H), 7.47–7.45 (m, 1H, Ar–H), 7.29 (d, J = 7.6 Hz, 1H, Ar–H), 7.27–7.21 (m, 2H, Ar–H), 6.98–6.95 (m, 1H, Ar–H), 6.66 (bs, 1H, Ar–H), 4.38 (dd, 1J = 11.0 Hz, 2J = 3.8 Hz, 1H, OCH₂), 4.07 (dd, 1J = 11.0 Hz, 2J = 6.5 Hz, 1H, OCH₂), 3.74 (m, 1H, CHOH), 3.18–3.16 (m, 4H, CH₂N piperazine); ¹³C NMR (101.0 MHz, DMSO-*d*₆) δ_C (ppm): 153.8, 148.9, 140.1, 130.5, 130.2–129.3 (q, 2J = 31.6 Hz), 126.0, 124.1–122.3 (q, 1J = 272.1 Hz), 117.9, 66.7, 64.1, 58.8, 52.6, 51.4, 45.5; ¹⁹F NMR (376.0 MHz, DMSO-*d*₆) δ_F (ppm): -60.14 (s, Ar–CF₃); HPLC-UV/HR-MS (ESI): for C₂₁H₂₃O₃ClF₃N₃ [M+H]⁺ calculated 458.1453 m/z , found 458.1471 m/z , Difference (ppm) -3.97; Purity (LC-UV/HR-MS): 98.84%.

1-[2-Hydroxypropyl-((3-trifluoromethyl)phenyl)carbamoyloxy]-4-(3,4-dichlorophenyl)piperazin-1-ium chloride (**6e**). Yield 2.41 g (46%); M_r 528.79; R_f 0.60; M_p 169–170 °C; IR (UATR): 3550 (ν OH), 3396 (ν NH), 2957 (ν_{as} CH₂), 2871 (ν_s CH₂), 1727 (ν C=O), 1605 (ν C=C), 1515 (δ NH), 1498 (ν CN), 1242 (ν_{as} C–O–C), 1150 (ν CF), 1062 (ν_s C–O), 1020 (δ_{ip} =C–H), 845 (δ_{oop} =C–H), 735 (γ C–Cl) cm⁻¹; ¹H NMR (400.0 MHz, DMSO-*d*₆) δ_H (ppm): 10.87 (s, 1H, NH⁺), 10.19 (s, 1H, NHCOO), 7.87 (s, 1H, Ar–H), 7.66–7.64 (m, 1H, Ar–H), 7.45–7.43 (m, 1H, Ar–H), 7.38–7.36 (m, 1H, Ar–H), 7.28–7.25 (m, 1H, Ar–H), 7.17–6.94 (m, 1H, Ar–H), 6.32 (bs, 1H, OH), 4.36 (dd, 1J = 11.0 Hz, 2J = 3.8 Hz, 1H, OCH₂), 4.05 (dd, 1J = 11.0 Hz, 2J = 6.5 Hz, 1H, OCH₂), 3.60 (m, 1H, CHOH), 3.17–3.13 (m, 4H, CH₂N piperazine); ¹³C NMR (101.0 MHz, DMSO-*d*₆) δ_C (ppm): 153.8, 149.8, 140.5, 132.2, 130.5, 130.2, 129.9–126.0 (q, 2J = 31.6 Hz), 126.0–121.3 (q, 1J = 272.1 Hz), 121.8, 117.5, 116.3, 66.7, 63.9, 58.7, 52.3, 51.2, 45.1, 42.3; ¹⁹F NMR (376.0 MHz, DMSO-*d*₆) δ_F (ppm): -60.18 (s, Ar–CF₃); HPLC-UV/HR-MS (ESI): for C₂₁H₂₂O₃Cl₂F₃N₃ [M+H]⁺ calculated 492.1063 m/z , found 492.1080 m/z , Difference (ppm) -3.45; Purity (LC-UV/HR-MS): 98.66%.

1-[2-Hydroxypropyl-((3-trifluoromethyl)phenyl)carbamoyloxy]-4-(3-trifluoromethylphenyl)piperazin-1-ium chloride (**6f**). Yield 1.77 g (34%); M_r 527.89; R_f 0.61; M_p 172–173 °C; IR (UATR): 3556 (ν OH), 3391 (ν NH), 2952 (ν_{as} CH₂), 2865 (ν_s CH₂), 1740 (ν C=O), 1605 (ν C=C), 1510 (δ NH), 1495 (ν CN), 1242 (ν_{as} C–O–C), 1152 (ν CF), 1062 (ν_s C–O), 1020 (δ_{ip} =C–H), 845 (δ_{oop} =C–H) cm⁻¹; ¹H NMR (400.0 MHz, DMSO-*d*₆) δ_H (ppm): 10.89 (s, 1H, NH⁺), 10.22 (s, 1H, NHCOO), 7.90 (s, 1H, Ar–H), 7.52–7.46 (m, 1H, Ar–H), 7.31–7.26 (d, J = 8.6 Hz, 1H, Ar–H), 7.23 (s, 1H, Ar–H), 7.11 (d, J = 7.5 Hz, 1H, Ar–H), 5.82 (bs, 1H, OH), 4.41 (dd, 1J = 11.0 Hz, 2J = 3.8 Hz, 1H, OCH₂), 4.10 (dd, 1J = 11.0 Hz, 2J = 6.5 Hz, 1H, OCH₂), 3.69 (m, 1H, CHOH), 3.11 (m, 4H, CH₂N piperazine); ¹³C NMR (101.0 MHz, DMSO-*d*₆) δ_C (ppm): 153.8, 150.9, 140.1, 131.3, 130.7, 130.6–130.4 (q, J = 32.6 Hz), 130.2–130.9, 126.2, 125.9–123.2 (q, J = 272.8 Hz), 122.3, 119.7, 116.2, 66.8, 64.1, 58.8, 52.5, 51.3, 45.3, 45.2, 42.8; ¹⁹F NMR (376.0 MHz, DMSO-*d*₆) δ_F (ppm): -60.17 (s, Ar–CF₃), -60.47 (s, Ar–CF₃); HPLC-UV/HR-MS (ESI): for C₂₂H₂₃O₃F₆N₃ [M+H]⁺ calculated 492.1716 m/z , found 492.1731 m/z , Difference (ppm) -3.05; Purity (LC-UV/HR-MS): 98.81%.

1-[2-Hydroxypropyl-((3-trifluoromethyl)phenyl)carbamoyloxy]-4-(4-diphenylmethyl)piperazin-1-ium chloride (**6g**). Yield 3.02 g (55%); M_r 550.02; R_f 0.64; M_p 179–180 °C; IR (UATR): 3550 (ν OH), 3396 (ν NH), 2957 (ν_{as} CH₂), 2871 (ν_s CH₂), 1727 (ν C=O), 1605 (ν C=C), 1512 (δ NH), 1495 (ν CN), 1244 (ν_{as} C–O–C), 1150 (ν CF), 1062 (ν_s C–O), 1020 (δ_{ip} =C–H), 845 (δ_{oop} =C–H) cm⁻¹; ¹H NMR (400.0 MHz, DMSO-*d*₆) δ_H (ppm): 10.46 (s, 1H, NH⁺), 10.19 (s, 1H, NHCOO), 7.90 (s, 1H, Ar–H), 7.69–7.67 (m, 1H, Ar–H), 7.60–7.40 (m, 1H, Ar–H), 7.40–7.17 (overlap, m, 11H, Ar–H), 5.90 (bs, 1H, OH), 4.41 (dd, 1J = 11.0 Hz, 2J = 3.8 Hz, 1H, OCH₂), 4.06 (dd, 1J = 11.0 Hz, 2J = 6.5 Hz, 1H, OCH₂), 3.47 (m, 1H, CHOH), 3.36–3.12 (m, 4H, CH₂N piperazine); ¹³C NMR (101.0 MHz, DMSO-*d*₆) δ_C (ppm): 153.8, 146.3, 142.5, 140.1, 130.5, 129.9, 129.3, 128.6, 128.0–119.3, 127.7, 127.2, 126.7, 126.0, 122.3, 119.3, 114.6, 74.3, 66.7, 63.9, 58.8, 53.1, 51.7, 48.2; ¹⁹F NMR (376.0 MHz, DMSO-*d*₆) δ_F (ppm): -60.17 (s, Ar–CF₃); HPLC-UV/HR-MS (ESI): for C₂₈H₃₀O₃F₃N₃ [M+H]⁺ calculated 514.2312 m/z , found 514.2337 m/z , Difference (ppm) -4.94; Purity (LC-UV/HR-MS): 98.85%.

The Extension of a Section 2.1.3 Determination of Some Physicochemical Properties in Main Article

• Estimation of Electronic Properties – The Details

The values of logarithms of molar absorption coefficients ($\log \varepsilon$) characterizing methanolic solutions of the compounds **6a–g** ($c = 5.0 \times 10^{-5}$ M) were observed at $\lambda_1 = 203.50\text{--}206.00$ nm, $\lambda_{2(\text{Ch-T})} = 238.50\text{--}243.00$ nm (charge-transfer absorption maximum) and $\lambda_3 = 279.50\text{--}286.50$ nm (Table 1 in Main Article), respectively, in a near UV (quartz) region of the electromagnetic spectrum between 190 nm and 400 nm [32]. The $\log \varepsilon$ values for observed absorption maxima (Table 1) were calculated according to a Lambert-Beer's law, which was expressed by Equation (S1) and explained briefly in [32], for example.

$$A = \varepsilon \times c \times l, \quad (\text{S1})$$

where the A parameter represented absorbance of a compound's solution, the ε descriptor was a molar absorption coefficient (in L/mol/cm units) and l was path length (in cm units).

• Estimation of Lipophilic Properties – The Details

Lipophilicity of prepared compounds **6a–g** was determined by reversed-phase high-performance liquid chromatography (RP-HPLC). Methanol (MeOH)/water mobile phases (MPs) with varying volume ratio of the organic modifier and water (60:40, 65:35, 70:30, 75:25, 80:20, 85:15 and 90:10 (v/v), respectively) were chosen. Retention factors (capacity factors; k) were calculated according to Equation (S2), methanolic solution of potassium iodine was used for dead time (t_d) determination.

$$k = (t_r - t_d)/t_d, \quad (\text{S2})$$

where t_r was retention time of a solute (in min), the t_d parameter denoted dead time of potassium iodine, an unretained analyte (in min).

The observed retention (t_r) and dead (t_d) times were means of three independent determinations and t_r values were listed in Table S1 and S2.

• Verification of Purity – The Details

The purity (in percentages) of analyzed compounds **6a–g** was verified by RP-HPLC. Areas of their peaks were measured using the MPH, which contained 90% proportion (v/v) of MeOH.

A2. The Extension of a Section 2.2. Biological Assays in Main Article

The Extension of a Section 2.2.1 In Vitro Antimycobacterial Evaluation in Main Article

• Determination of a Minimum Inhibitory Concentration (MIC) Against *Mtb* H₃₇R_a – The Details

The *mycobacterium* was grown on Middlebrook broth (MB; MiddleBrook Pharmaceuticals, Inc., Westlake, TX, USA), supplemented with Oleic-Albumin-Dextrose-Catalase (OADC) supplement (Difco, Lawrence, KS, USA) and salicylate-derived mycobactin J (2 $\mu\text{g/mL}$; Allied Monitor Inc., Fayette, MO, USA), an iron-binding siderophore [35,36].

At log phase growth, a culture sample (10 mL) was centrifuged at 15,000 rpm/20 min using a bench top centrifuge MPW-65R (MPW Med Instruments, Warsaw, Poland). Following removal of the supernatant, a pellet was washed in fresh liquid Middlebrook 7H9GC broth (MiddleBrook Pharmaceuticals, Inc.) and re-suspended in a fresh OADC-supplemented MB (10 mL).

Turbidity was adjusted to match the McFarland standard No. 1 [37] containing approximately 3×10^8 Colony Forming Units (CFU) with MB broth. Further 1:20 dilution of the culture was performed in MB broth. Susceptibility of *Mtb* H₃₇R_a was investigated in a 96-well plate format. In the experiments, sterile deionized water (300 μL) was added to all outer-perimeter wells of the plates to minimize evaporation of the medium in test wells during incubation. Particular substance (100 μL) was incubated with *Mtb* H₃₇R_a (100 μL). The dilutions of each tested compound, i.e., **6a–g** and INH reference drug, respec-

tively, were prepared in triplicate and final concentrations varied from 1000 µg/mL to 1 µg/mL. All molecules were dissolved in DMSO (Sigma-Aldrich, Irvine, UK), and dilutions were made in supplemented MB broth. The plates were sealed with parafilm and incubated at 37 °C for 7 days.

Following incubation, 10% addition a water-soluble dye, the alamarBlue reagent (AbD Serotec, Kidlington, UK), was mixed into each well. This resaurin-based reagent served as an oxidation-reduction indicator of a metabolic function and cellular health in cell viability bioassays [38].

Absorbance readings at $\lambda = 570$ nm and 600 nm were taken, initially for background subtraction and after 24h re-incubation. The subtraction is necessary for strongly colored compounds, where the color may interfere with the interpretation of any color change. For non-interfering compounds, a blue color in a well was interpreted as absence of growth and pink color was scored as growth [39,40].

The *MIC* value was defined as the lowest concentration of a compound, at which no visible bacterial growth was observed. In other words, *MIC* was the lowest concentration that prevented visual color change from blue to pink. The *MIC* value has been routinely and widely used in bacterial assays and it has been a standard detection limit according to the Clinical and Laboratory Standards Institute (CLSI) [39,40]. The estimated *MIC* values (in µM units) were provided in Table 3 (Main Article).

● *Determination of a Minimum Inhibitory Concentration (MIC) Against MK DSM, MS and MM – The Details*

Broth dilution micromethod in Middlebrook 7H9 medium (Difco, Lawrence, MO, USA) supplemented with BD BBL Middlebrook OADC Enrichment medium (Becton, Dickinson & Company, Franklin Lakes, NJ, USA) containing 8.5 g NaCl, 50.0 g bovine albumin (fraction V), 20.0 g dextrose, 0.03 g catalase, and 0.6 mL oleic acid [41], respectively, was used to determine the *MIC* values for given strains, as described [42].

Tested molecules (**6a–g**, INH) were dissolved in DMSO (Sigma-Aldrich, Irvine, UK) and final concentration of DMSO did not exceed 2.5% of the total solution composition. The final concentrations, varying from 1000 µg/mL to 1 µg/mL, were obtained by a two-fold serial dilution of a stock solution in a microtiter plate with sterile medium.

Bacterial inocula were prepared by transferring colonies from culture into sterile water. Cell density was adjusted to the 0.5 McFarland units [37] using the cell density meter Densi-La-Meter (LIAP, Riga, Latvia). Final inoculum was made by 1:1000 dilution of the suspension with sterile water. Drug-free controls, sterility controls and controls consisted of medium and DMSO alone were included. Results were determined visually after static incubation in the darkness in aerobic atmosphere for: (i) 3 days at 37 °C in a case of *MS* susceptibility testing; (ii) 7 days at 37 °C (*MK DSM*) and (iii) 21 days at 28 °C (*MM*), respectively.

The *MIC* parameter was defined as the lowest concentration of a compound, at which no visible bacterial growth was observed. The *MIC* value has been routinely and widely used in bacterial assays considering it a standard detection limit according to CLSI [39,40]. The observed *MIC* values (in µM units) are provided in Table 3 (Main Article).

The Extension of a Section 2.2.2 *In Vitro* Cytotoxicity Screening in Main Article

The human Caucasian hepatocyte carcinoma cell line HepG2, obtained from the American Type Culture Collection (ATCC Number: HB-8065), was cultured on 100 mm dishes in 5% CO₂ humidified atmosphere at 37 °C in Dulbecco's Modified Eagle's Medium (DMEM; Biosera, Nuaille, France) containing 10% fetal bovine serum (Biocrom AG, Berlin, Germany) and 0.2% (*v/v*) of penicillin/streptomycin solution. DMEM is a broadly used basal medium supporting the growth of numerous mammalian cells.

The cultivation was carried out in 100 mm-dishes, the number of cell passages was from 10 to 25. The cells were trypsinised to detach, centrifuged using a Biosan LMC-3000 centrifuge (Biosan, Riga, Latvia), resuspended, seeded at 70% confluency and grown in 24-well culture plates for 24 h.

The compounds **6a–g** were dissolved in DMSO (Merck Life Science, Bratislava, Slovakia) and the cells were incubated with increased concentration ($c = 0\text{--}60\ \mu\text{M}$) of these (potential) inhibitors for 24 h. At the end of incubation period, the cell proliferation was evaluated by the Janus Green B assay following a procedure of Raspotnig et al. [43] with appropriate modifications [44]. Briefly, culture medium was removed from cell layers by vacuum aspiration and these layers were fixed in 50% ethanol (CentralChem, Bratislava, Slovakia) for 30 min, followed by vacuum aspiration of the fixative.

Finally, fixed cell layers were stained with a 0.2% solution of purified Janus Green B (Sigma-Aldrich, Steinheim, Germany), chemically 3-diethylamino-7-(4-dimethylamino-phenylazo)-5-phenylphenazin-1-ium chloride, in phosphate-buffered saline (PBS solution) without Ca^{2+} or Mg^{2+} ions (Biochrom, Berlin, Germany) for 3 min at room temperature. After immediate removal of the stain using a Spectrum Vacu/Trol vacuum water aspirator (Fisher Scientific, Vienna, Austria), the whole plate was washed twice in cold water and eluted from cell layers by the 0.5 mL addition of 0.5 M HCl. The plate was read with an Epoch Biotek microplate reader (Epoch Biotek U.S., Winooski, VT, USA) against 0.5 M HCl blank at $\lambda = 595\ \text{nm}$. The cell count was calculated using a calibration curve representing the dependency of absorbance (A) at $\lambda = 595\ \text{nm}$ on HepG2 cell density. Each experiment was performed three-fold in duplicates [43,44].

A3. The Extension of a Section 2.3 In Silico Evaluation of Synthesized Bases in Main Article

No additional information is necessary to provide in this section.

A4. The Extension of a Section 2.4 Calculations and Statistical Analyses in Main Article

The calculated descriptors were as follows: logarithms of extrapolated retention factors ($\log k_w$), slope (S), reduced chi-square (χ^2_{red}), residual sum of squares (RSS), correlation coefficient (R), adjusted coefficient of determination ($Adj. R^2$), root mean squared error (standard deviation; $RMSE$), Fisher's significance ratio (Fisher's F -test; F) and probability of obtaining F Ratio (significance of a whole model; $Prob > F$), respectively (Table 2 in Main Article). The number of points (number of cases; n) was 7.

The analyses were also focused on indication of a significance level of calculated F Ratio as follows: * (one star) – statistically significant, ** (two stars) – statistically very significant, *** (three stars) – statistically extremely significant (Table 2). Detailed information regarding given statistical descriptors could be found in a research paper [47], for example.

The chemometric principal component analysis (PCA) tool was used to explore relationships between values of estimated analytical and physicochemical descriptors (m/z_{measured} , $\log \varepsilon_2(\text{Ch-T})$ and $\log k_w$) as well as $\log (1/\text{MIC} [\text{M}])$ and $\log (1/\text{IC}_{50} [\text{M}])$ parameters derived from both MIC and IC_{50} data sets. The sets were connected with in vitro biological (antimycobacterial and cytotoxic) activities of the compounds **6a–g**. The calculated descriptors (I_{GPI} , I_{MPI} , I_{CADT} , I_{B} , I_{P} , I_{T} and I_{QTP}) related to corresponding bases (**5a–g**) were also involved in the analyses.

PCA refers to the problem of fitting a low-dimensional affine subspace to a set of data points in high-dimensional space. The mathematical PCA tool aims to represent the variation present in the dataset (i.e., responses used to characterize samples) using a small number of factors (Figure 6a and 6b in Main Article).

For visual analysis, two-dimensional (2D) projection of the samples was constructed having axes (principal components, PCs) as the factors (Figure 6a). Each PC was a linear combination of the original responses (that retained some correlation among) and PCs were orthogonal to each other. PCs iteratively calculated hold as much variation from original data set as possible, in a way that PC 1 explained more the data variation than PC 2, and PC 2 explain more data variation than PC 3 [48].

All analyzed parameters were given on the same scale. Thus, several data pre-treatment methods were investigated, i.e., standardized and centered transformation procedures as well as Pareto scaling were applied, as published in [49]. The resulting values of all relevant PCA-based descriptors, but not the values of transformed variables,

were the same if considering all rescaling techniques provided above. The proper definitions and meaning of the terms used in current research are given below.

Scree plot (not provided) is used to plot eigenvalues (λ_e) according to their size and visualize if there was a point in this graph such that the slope of the graph went from 'steep' to 'flat' and to keep only the components, which were before the elbow.

The λ_e parameter associated to a component is equal to the sum of squared factor scores for this component. The Kaiser–Guttman rule is considered the most common stopping rule in PCA [50], which is aimed at an average value of $\lambda_e > 1.00$.

Circle of correlation (Figure 6b) is a set of points, the sum of squared coordinates, which is equal to a constant. Consequently, when the data are perfectly represented by only two components, the sum of squared loadings is equal to one, and therefore, in this case, the loadings are positioned on the circle.

Pearson's correlation coefficient (r) is a measure of the strength of a linear relationship between two variables, which indicates a positive or negative correlation as a measure of reliability [51].

Current PCA was performed by the XLSTAT software, ver. 2016.02.28451 (Addinsoft, New York, NY, USA), a cloud-based statistical application for statistics and data analyses, which worked as an add-on to the Microsoft Excel software, ver. 2016 (Microsoft Corp., Redmont, WA, USA).

A5. The Extension of a Section 3.3. *In Silico* Evaluation of Synthesized Bases in Main Article

• The Criteria for Prediction of a Specific Activity

The highest values were calculated for I_{GPI} and I_B (Table S3). Theoretically, if these parameters were relatively high, particular compounds, for which these descriptors were generated, might be close analogues of known biologically effective molecules. Thus, if interested in finding new leads, a better way would be to choose the compounds, for which specified activity was predicted with relatively lower probability [45,46], for example, $0.450 < \text{probability of a compound being biologically active (specific descriptor)} < 0.720$.

• The Probability to Act as Anticancer Agents

The probability that investigated bases (**5a–g**) would act as anticancer agents ($I_{CADT} = 0.287\text{--}0.368$) was lower compared to their eventual potential being effective general pump inhibitors ($I_{GPI} = 0.573\text{--}0.707$), or membrane permeability inhibitors ($I_{MPI} = 0.457\text{--}0.555$).

• The Probability to Cause Unwanted Cardiovascular Effects

The presence of a (substituted) 4-phenylpiperazin-1-yl moiety was mirrored in higher probability to cause bradycardia, as I_{GPI} values in the interval from 0.673 (**5c**) to 0.724 (**5a**) indicated (Table S3). Less probable would be that **5a–g** could cause palpitation ($I_P = 0.371\text{--}0.432$), prolongation of a QT-interval ($I_{QTP} = 0.362\text{--}0.640$), or tachycardia ($I_T = 0.360\text{--}0.454$).

A6. The Extension of a Section 3.4. Structure–Activity Relationships in Main Article

• The Differences in Compounds' Properties Described with Both Principal Component 1 and Principal Component 2

The molecules with the highest $\log \varepsilon_{2(\text{Ch-T})}$ as well as $\log k_w$ values (**6e–g**) were defined by a negative PC 1 ($\text{PC } 1 \leq -0.286$). In fact, electronic properties of investigated compounds were not optimally described with PC 2 in a two-dimensional (2D) score plot (Figure 6a in Main Article) constructed on a PC 1 \times PC 2 coordinate system. The highest contributions to $\log \varepsilon_{2(\text{Ch-T})}$ (vector B) were noted for PC 4 (30.38%), PC 6 (19.22%) and PC 1 (6.21%), respectively.

The $\log k_w$ variable (C) was described with both PC 1 (7.70%) and PC 2 (10.34%) more precisely (Table S5). The more positive PC 1 values were, the lower lipophilicity of analyzed compounds was.

In fact, PC 2 could not be regarded as the optimal descriptor to characterize in vitro cytotoxic properties of tested substances, with the contribution of 0.55% only. The con-

tribution of first three variables to this component was more notable as follows: PC 4 (29.67%), PC 1 (6.97%) and PC 6 (3.02%), respectively.

- *The Indication of Variables*

The letter A indicated an analytical m/z_{measured} variable from HPLC-UV/HR-MS and digit 1 labeled the vector, which was constructed on calculated $\log(1/\text{MIC} [\text{M}])$ values. These MIC parameters resulted from the in vitro screening of **6a–g** against *Mtb* H₃₇R_a. The labeling of other vectors was based on an analogical principle as follows: B ($\log \varepsilon_{2 (\text{Ch-T})}$), C ($\log k_w$), I_{GPI} (connected with the in silico I_{GPI} variable), I_{MPI} (I_{MPI}), I_{CADT} (I_{CADT}), I_{B} (I_{B}), I_{P} (I_{P}), I_{T} (I_{T}), I_{QTP} (I_{QTP}), 2 (MK DSM), 3 (MS), 4 (MM), and 5 (vector built on calculated $\log(1/\text{IC}_{50} [\text{M}])$ values. These IC_{50} values resulted from the in vitro screening of **6a–g** against the HepG2 cell line), respectively.

- *The Relationships Between Investigated Parameters and Probability to Act as Anticancer Agents for the Bases (5a–g)*

The increase in m/z_{measured} values of investigated salts might hypothesize that corresponding bases (**5a–g**) could not be promising anticancer drugs (I_{CADT} ; $r = -0.8269$). Higher $\log \varepsilon_{2 (\text{Ch-T})}$ values of the **6a–g** set proposed that corresponding bases (**5a–g**) could not be regarded as the most promising drugs for the treatment of cancer (I_{CADT} ; $r = -0.7438$).

B. Tables

Table S1. Retention times t_r and lipophilicity indices $\log k$ (RP-HPLC) of **6a–g** determined in the mobile phases with a various volume ratio (v/v) of a methanol (MeOH) organic modifier and water, i.e., from 60:40 to 70:30.

Entry	Mobile phase MeOH/water (v/v)					
	60:40		65:35		70:30	
	t_r (min)	$\log k$	t_r (min)	$\log k$	t_r (min)	$\log k$
6a	9.8460	1.3202	4.843	1.0121	2.5430	0.7323
6b	16.1710	1.5357	7.5001	1.2020	3.7102	0.8964
6c	10.5670	1.3509	5.0610	1.0312	2.5650	0.7361
6d	17.8115	1.5777	9.8600	1.3209	4.6270	0.9923
6e	24.7159	1.7372	13.5197	1.4579	7.1077	1.1787
6f	26.5828	1.7516	13.6400	1.4618	5.8650	1.0952
6g	23.1377	1.6913	11.4669	1.3864	6.4010	1.1000

Table S2. Retention times t_r and lipophilicity indices $\log k$ (RP-HPLC) of **6a–g** determined in the mobile phases with a various volume ratio (v/v) of a methanol (MeOH) organic modifier and water, i.e., from 75:25 to 90:10.

Entry	Mobile phase MeOH/water (v/v)							
	75:25		80:20		85:15		90:10	
	t_r (min)	$\log k$	t_r (min)	$\log k$	t_r (min)	$\log k$	t_r (min)	$\log k$
6a	1.4250	0.4808	0.8180	0.2397	0.5370	0.0570	0.3672	−0.1087
6b	1.9730	0.6221	1.0810	0.3608	0.6510	0.1406	0.4170	−0.0529
6c	1.4120	0.4734	0.8041	0.2322	0.4942	0.0207	0.3473	−0.1327
6d	2.3280	0.6940	1.2002	0.4062	0.7073	0.1764	0.4363	−0.0335
6e	3.9380	0.9223	1.8850	0.6023	0.9892	0.3222	0.5672	0.0806
6f	4.1111	0.9409	2.0902	0.6472	1.0574	0.3512	0.6570	0.1445
6g	2.7360	0.7641	1.3290	0.4505	0.7240	0.1867	0.4221	−0.0477

Table S3. The prediction of probability for the bases (**5a–g**) to act as general pump inhibitors (I_{GPI}) and membrane permeability inhibitors (I_{MPI}) as well as drugs for the treatment of cancer-associated diseases (I_{CADT}). The calculation of probability that these molecules might cause bradycardia (I_B), palpitation (I_P), tachycardia (I_T), and prolongation of a QT interval (I_{QTp}).

Entry	I_{GPI}	I_{MPI}	I_{CADT}	I_B	I_P	I_T	I_{QTp}
5a	0.613	0.535	0.367	0.724	0.432	0.452	0.433
5b	0.596	0.553	0.368	0.705	0.375	0.454	0.362
5c	0.576	0.470	0.363	0.673	0.427	0.360	0.491
5d	0.582	0.555	0.354	0.693	0.411	0.445	0.523
5e	0.573	0.517	0.344	0.717	0.392	0.447	0.558
5f	0.598	0.547	0.351	0.674	0.400	0.430	0.405
5g	0.707	0.457	0.287	0.522	0.371	0.605	0.640

Table S4. The selectivity index (SI) values of in vitro evaluated compounds **6a–g**, which were calculated as $SI = IC_{50}$ (in μM units)/MIC (in μM units). The IC_{50} s indicated toxicity in human liver hepatocellular carcinoma (HepG2) cells, the MICs were determined against *M. tuberculosis* H37Ra ATCC 25177 (*Mtb* H37Ra), *M. kansasii* DSM 44162 (MK DSM), *M. smegmatis* ATCC 700084 (MS), and *M. marinum* CAMP 5644 (MM).

Entry	SI			
	<i>Mtb</i> H37Ra	MK DSM	MS	MM
6a	1.19	1.19	0.60	1.19
6b	0.98	0.98	0.49	0.98
6c	1.47	0.74	0.37	0.74
6d	1.34	5.36	0.67	2.87
6e	7.78	1.94	0.97	1.94
6f	3.61	3.61	3.61	1.80
6g	6.11	1.53	1.63	2.74

Table S5. The contribution of evaluated variables (in percentages) to particular principal components (PCs; PC 1–6).

¹ Variable	PC 1	PC 2	PC 3	PC 4	PC 5	PC 6
A	8.66	0.93	2.90	6.67	2.86	6.90
B	6.21	0.05	1.14	30.38	5.09	19.22
C	7.70	10.34	0.00	1.74	0.24	0.31
I_{GPI}	5.23	12.00	19.59	0.18	2.09	0.18
I_{MPI}	2.07	26.94	11.75	1.96	6.50	1.92
I_{CADT}	9.19	4.19	0.02	0.27	1.16	0.43
I_B	6.58	10.11	1.47	1.13	0.79	25.20
I_P	6.01	3.95	10.35	17.13	9.24	0.69
I_T	7.12	1.93	17.13	0.00	6.31	10.43
I_{QTP}	5.50	5.25	22.46	0.02	12.35	6.84
1	8.32	0.37	7.95	0.61	11.25	4.22
2	4.42	16.41	2.02	0.52	22.69	5.12
3	7.49	3.99	0.99	8.63	5.62	13.87
4	8.55	3.00	0.84	1.11	11.13	1.69
5	6.97	0.55	1.39	29.67	2.69	3.02

¹ The indication of investigated variables is as follows: A (vector assigned to the $m/z_{measured}$ variable), B ($\log \varepsilon_{2(CH-T)}$), C ($\log k_w$), I_{GPI} (connected with the I_{GPI} variable describing analyzed bases **5a–g**), I_{MPI} (I_{MPI}), I_{CADT} (I_{CADT}), I_B (I_B), I_P (I_P), I_T (I_T), I_{QTP} (I_{QTP}), 1 (vector built on the $\log (1/MIC [M])$ values. These MIC parameters resulted from the in vitro screening of **6a–g** against *Mtb* H37Ra), 2 (MK DSM), 3 (MS), 4 (MM), and 5 (vector built on the $\log (1/IC_{50} [M])$ values. These IC_{50} values resulted from the in vitro screening of **6a–g** against the HepG2 cell line), respectively.

C. Figures – NMR and HPLC-UV/HR-MS Spectra of Final Compounds

C1. ^1H NMR, ^{13}C NMR, ^{19}F NMR and HPLC-UV/HR-MS (ESI) Spectra of 1-[2-Hydroxypropyl]-[(3-trifluoromethyl)phenyl]carbamoyloxy]-4-phenylpiperazin-1-ium Chloride (6a)

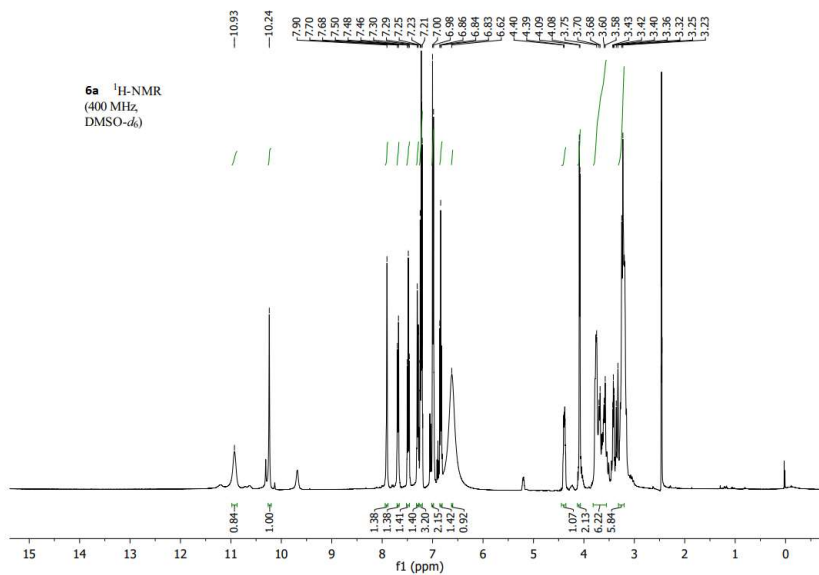


Figure S1. ^1H NMR Spectrum of the compound 6a.

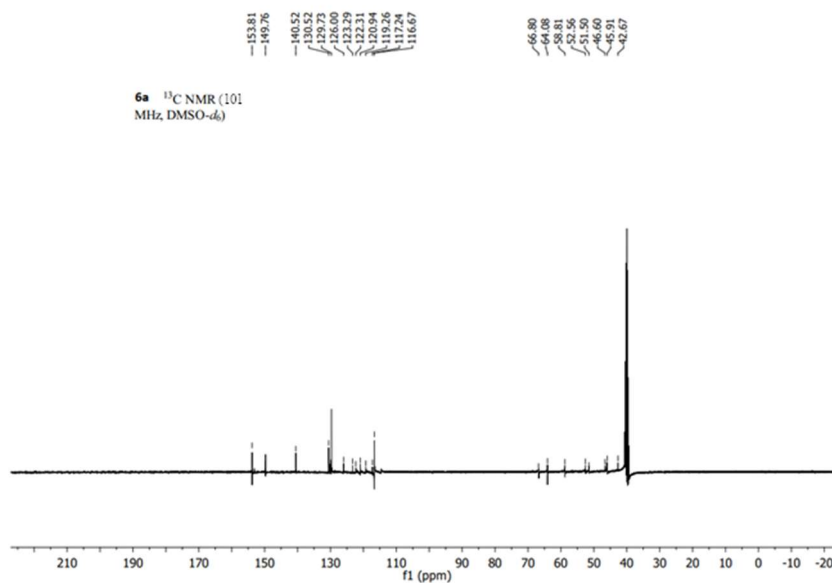


Figure S2. ^{13}C NMR Spectrum of the compound 6a.

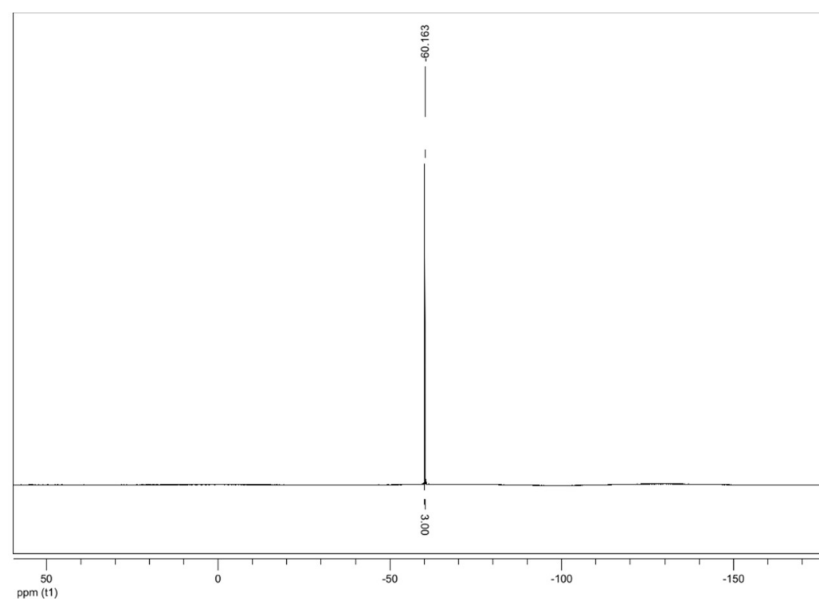


Figure S3. ^{19}F NMR Spectrum of the compound 6a.

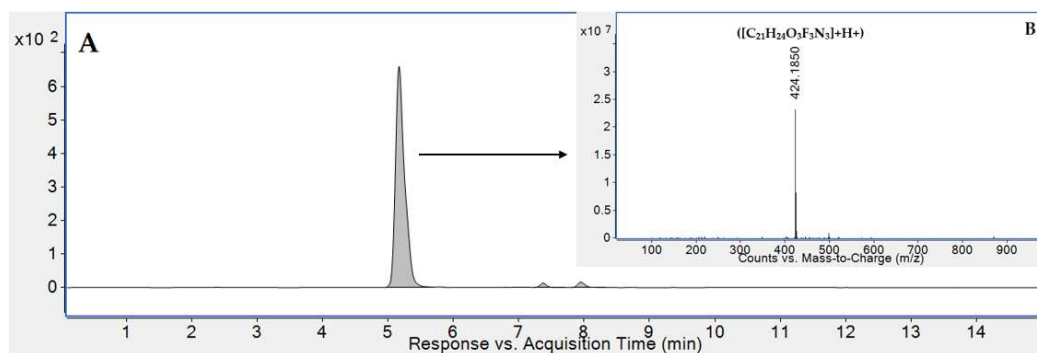


Figure S4. LC-UV-MS analysis of the compound 6a. Panel A – purity profile (LC-UV –254 nm), panel B – HR-MS spectrum of the desired compound (the major peak from UV chromatogram).

C2. ^1H NMR, ^{13}C NMR, ^{19}F NMR and HPLC-UV/HR-MS (ESI) Spectra of 1-[2-Hydroxypropyl]-[(3-trifluoromethyl)phenyl]carbamoyloxy]-4-(4-methylphenyl)-piperazin-1-ium Chloride (6b**)**

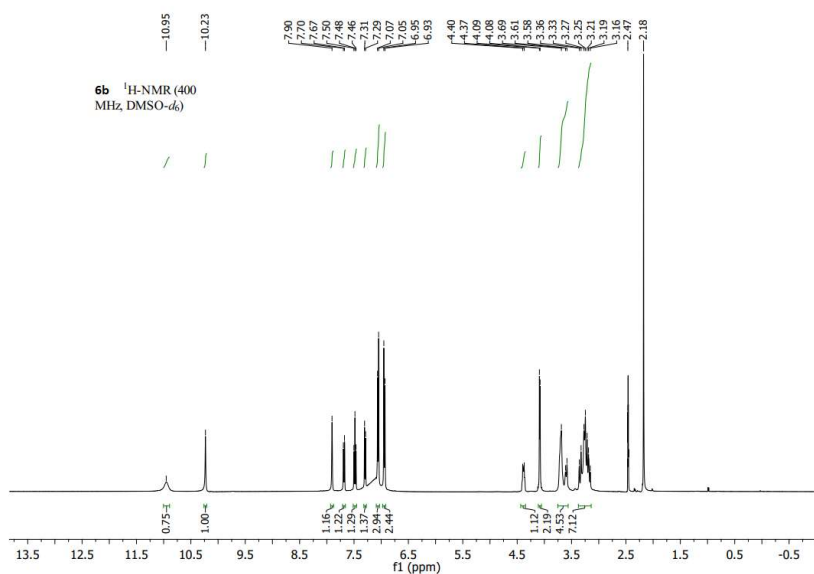


Figure S5. ^1H NMR Spectrum of the compound **6b**.

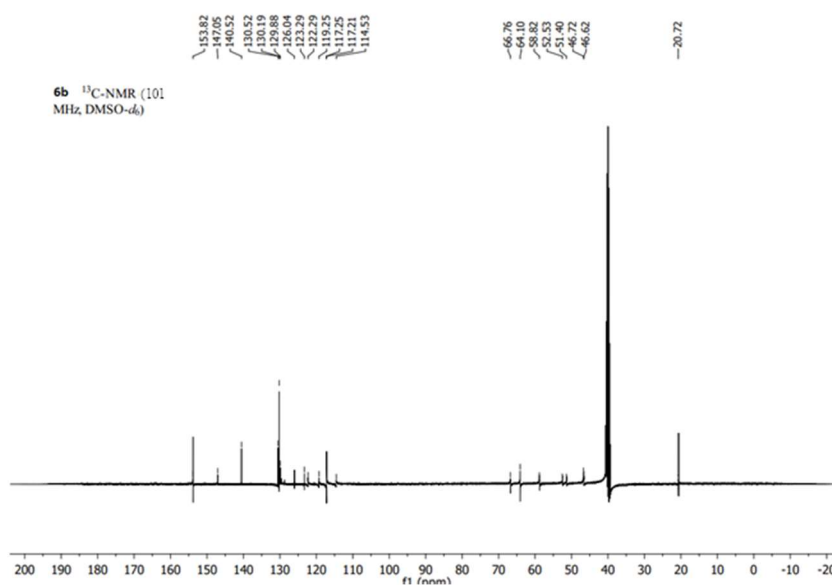


Figure S6. ^{13}C NMR Spectrum of the compound **6b**.

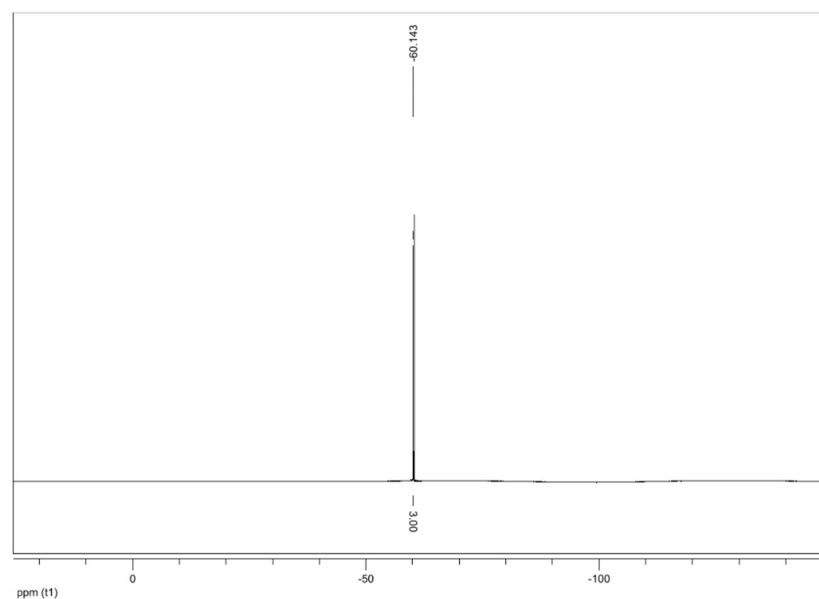


Figure S7. ^{19}F NMR Spectrum of the compound **6b**.

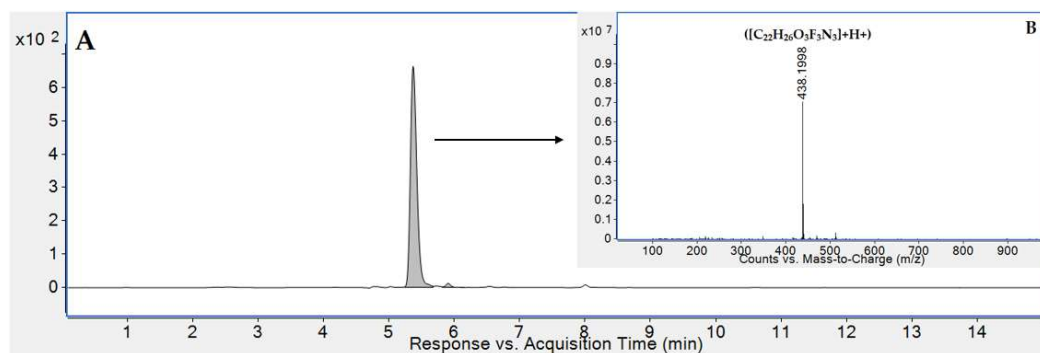


Figure S8. LC-UV-MS analysis of the compound **6b**. Panel A – purity profile (LC-UV –254 nm), panel B – HR-MS spectrum of the desired compound (the major peak from UV chromatogram).

C3. ^1H NMR, ^{13}C NMR, ^{19}F NMR and HPLC-UV/HR-MS (ESI) Spectra of 1-[2-Hydroxypropyl]-[(3-trifluoromethyl)phenyl]carbamoyloxy]-4-(4-fluorophenyl)-piperazin-1-ium Chloride (6c)

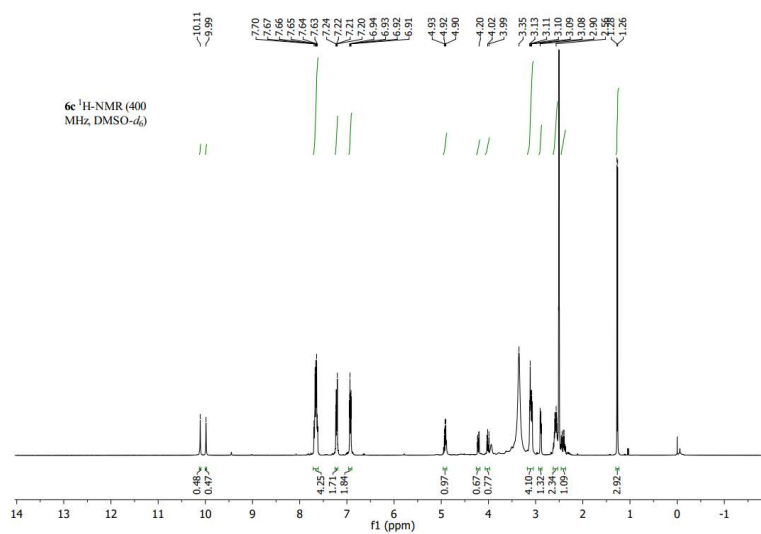


Figure S9. ^1H NMR Spectrum of the compound **6c**.

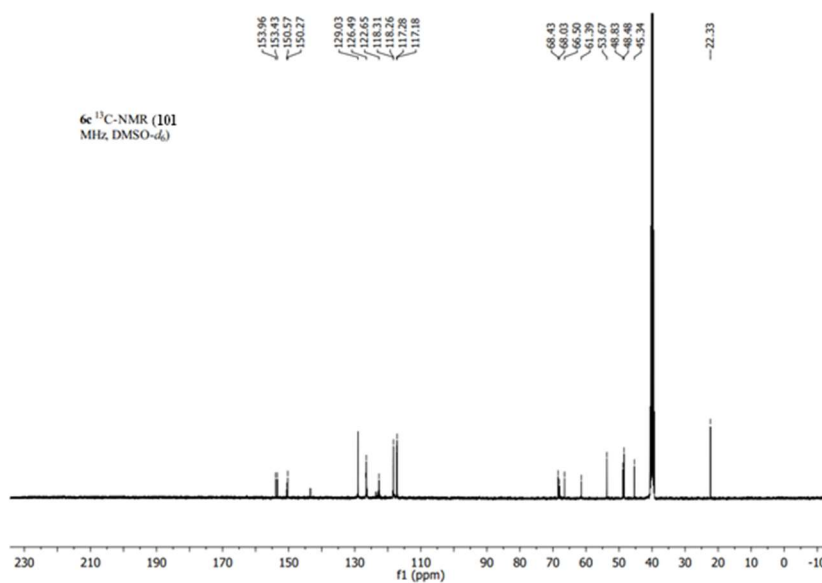


Figure S10. ^{13}C NMR Spectrum of the compound **6c**.

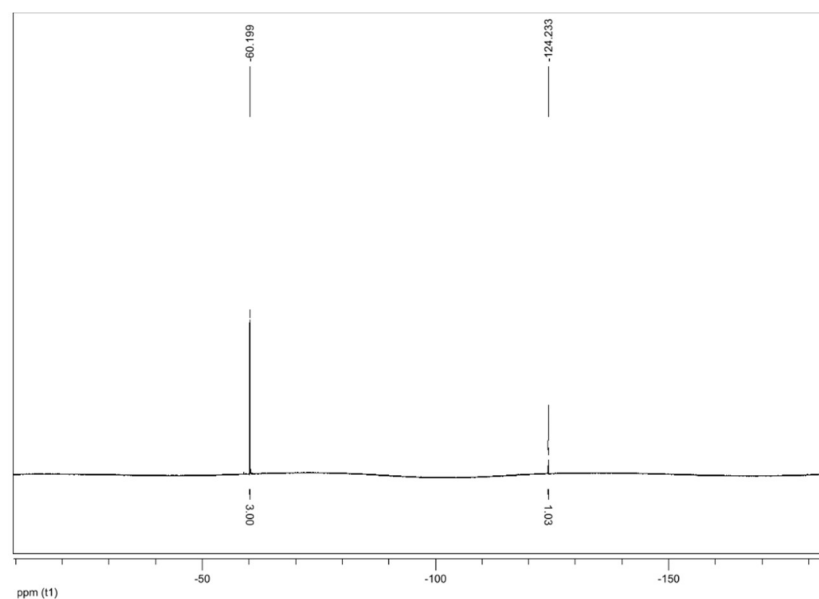


Figure S11. ^{19}F NMR Spectrum of the compound **6c**.

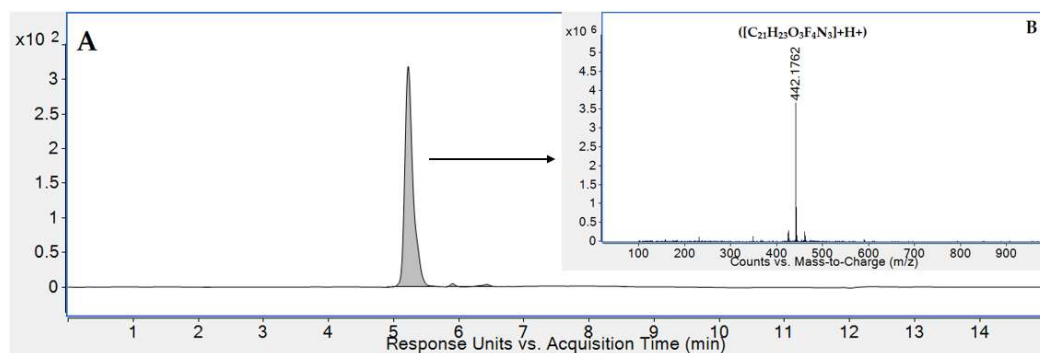


Figure S12. LC-UV-MS analysis of the compound **6c**. Panel A – purity profile (LC-UV –254 nm), panel B – HR-MS spectrum of the desired compound (the major peak from UV chromatogram).

C4. ^1H NMR, ^{13}C NMR, ^{19}F NMR and HPLC-UV/HR-MS (ESI) Spectra of 1-[2-Hydroxypropyl]-[(3-trifluoromethyl)phenyl]carbamoyloxy]-4-(4-chlorophenyl)-piperazin-1-ium Chloride (6d)

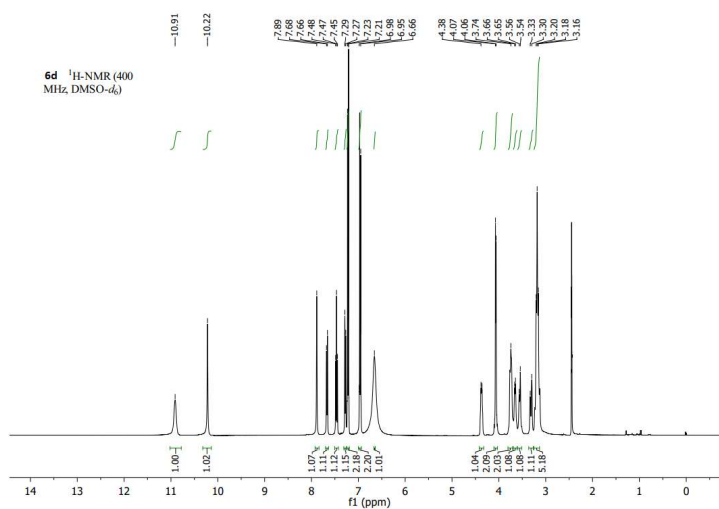


Figure S13. ^1H NMR Spectrum of the compound **6d**.

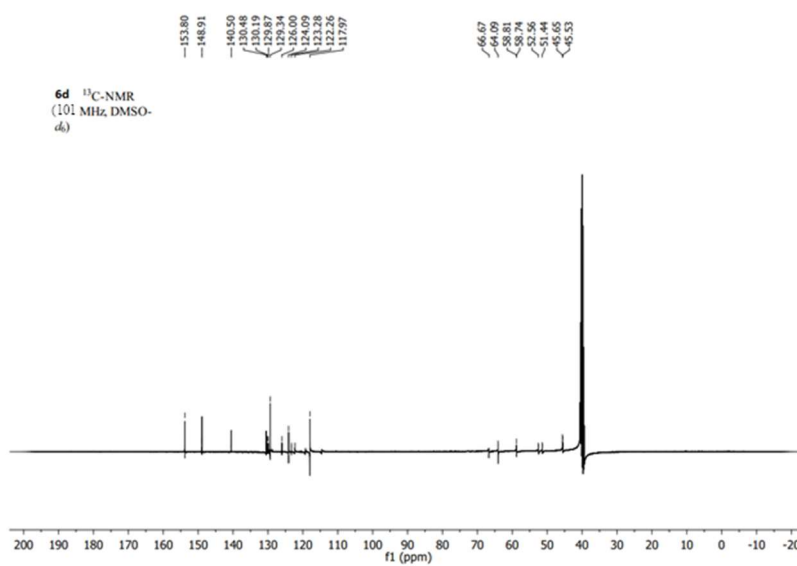


Figure S14. ^{13}C NMR Spectrum of the compound **6d**.

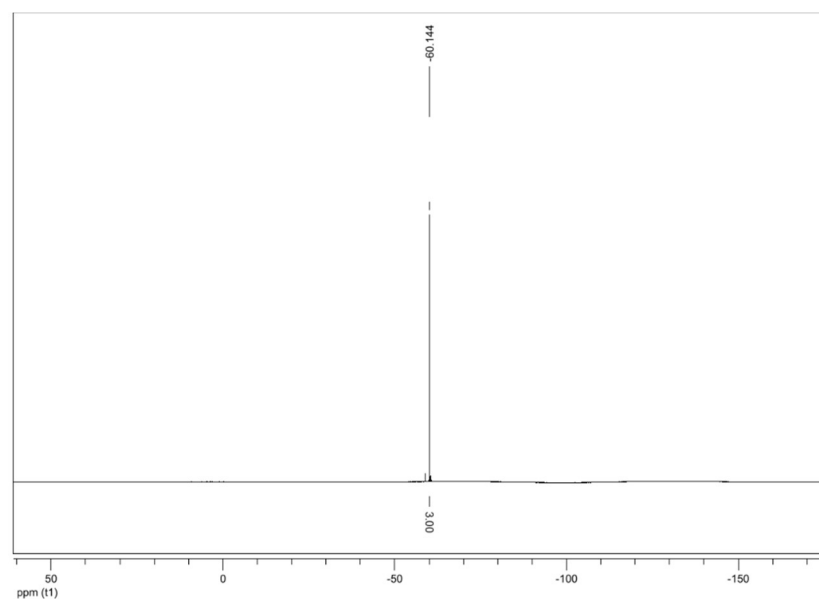


Figure S15. ^{19}F NMR Spectrum of the compound **6d**.

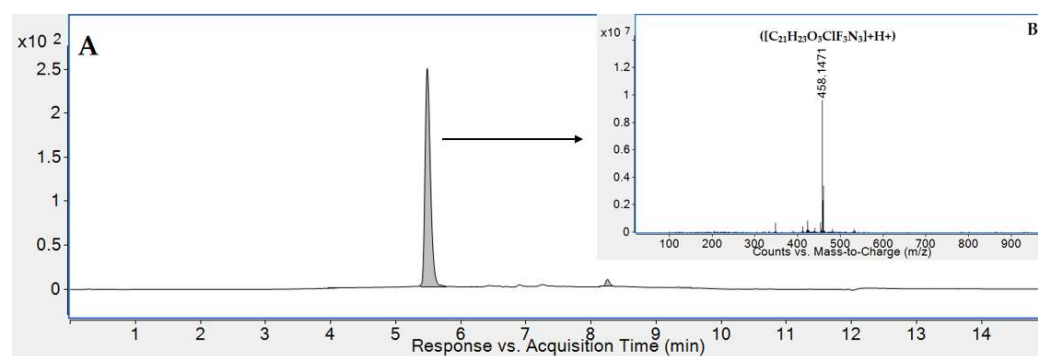


Figure S16. LC-UV-MS analysis of the compound **6d**. Panel A – purity profile (LC-UV –254 nm), panel B – HR-MS spectrum of the desired compound (the major peak from UV chromatogram).

C5. ^1H NMR, ^{13}C NMR, ^{19}F NMR and HPLC-UV/HR-MS (ESI) Spectra of 1-[2-Hydroxypropyl]-[(3-trifluoromethyl)phenyl]carbamoyloxy]-4-(3,4-dichlorophenyl)-piperazin-1-ium Chloride (**6e**)

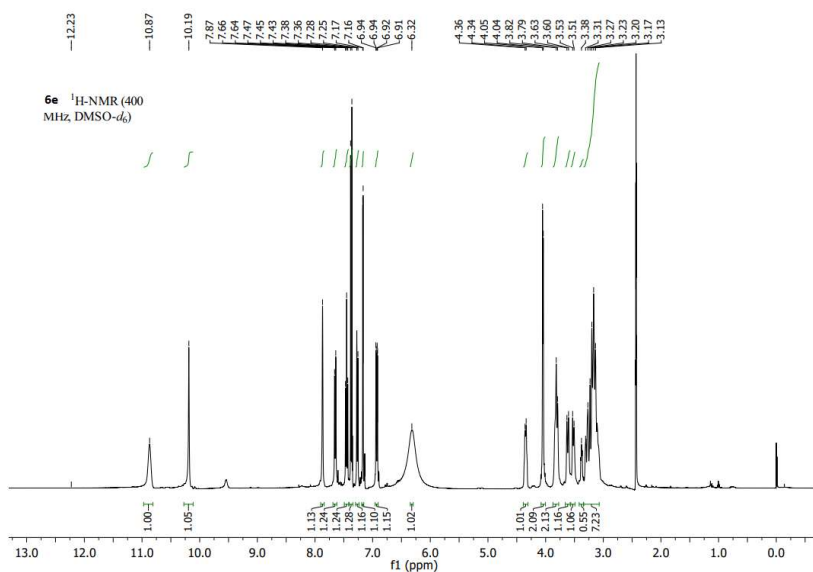


Figure S17. ^1H NMR Spectrum of the compound **6e**.

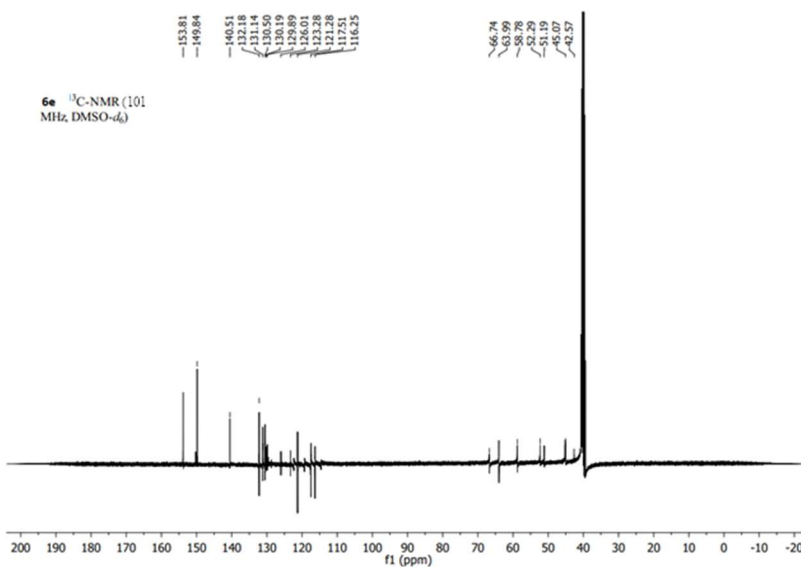


Figure S18. ^{13}C NMR Spectrum of the compound **6e**.

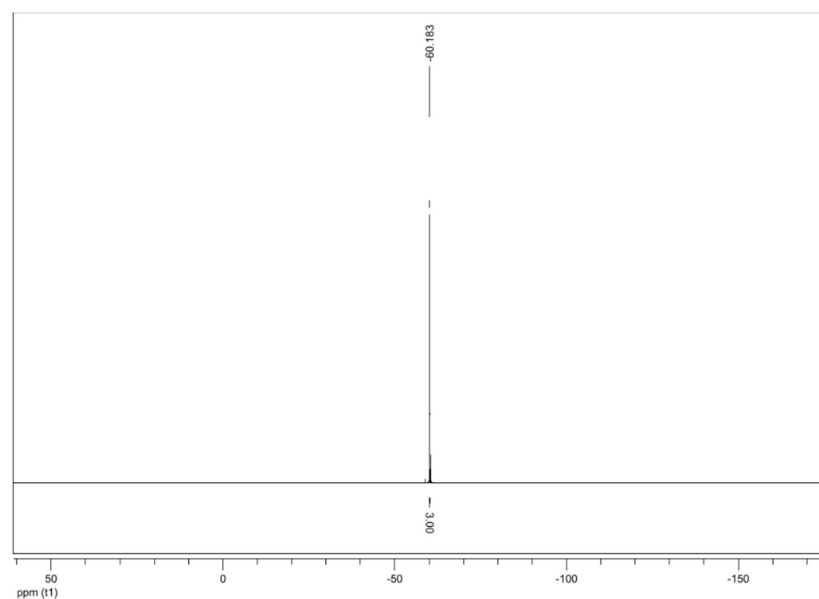


Figure S19. ^{19}F NMR Spectrum of the compound **6e**.

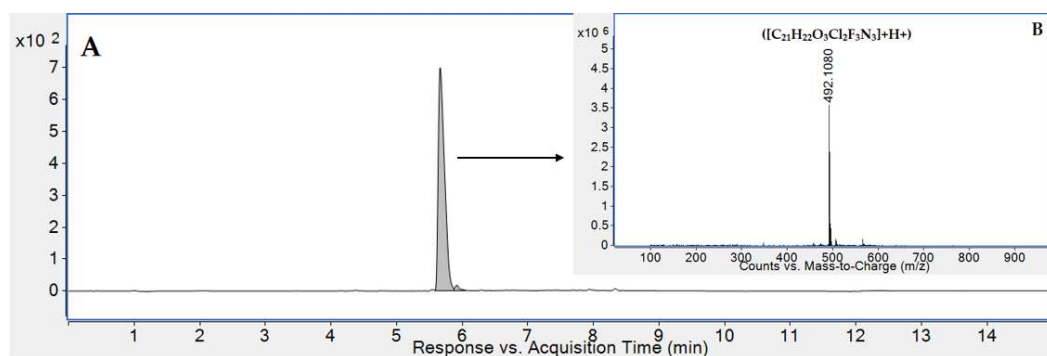


Figure S20. LC-UV-MS analysis of the compound **6e**. Panel A – purity profile (LC-UV –254 nm), panel B – HR-MS spectrum of the desired compound (the major peak from UV chromatogram).

C6. ^1H NMR, ^{13}C NMR, ^{19}F NMR and HPLC-UV/HR-MS (ESI) Spectra of 1-[2-Hydroxypropyl]-[(3-trifluoromethyl)phenyl]carbamoyloxy]-4-(3-trifluoromethyl-phenyl)piperazin-1-ium Chloride (6f)

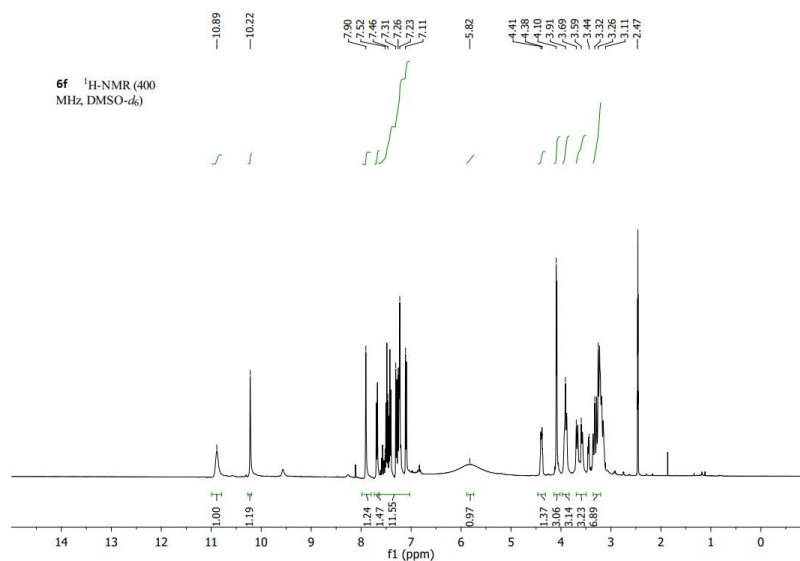


Figure S21. ^1H NMR Spectrum of the compound 6f.

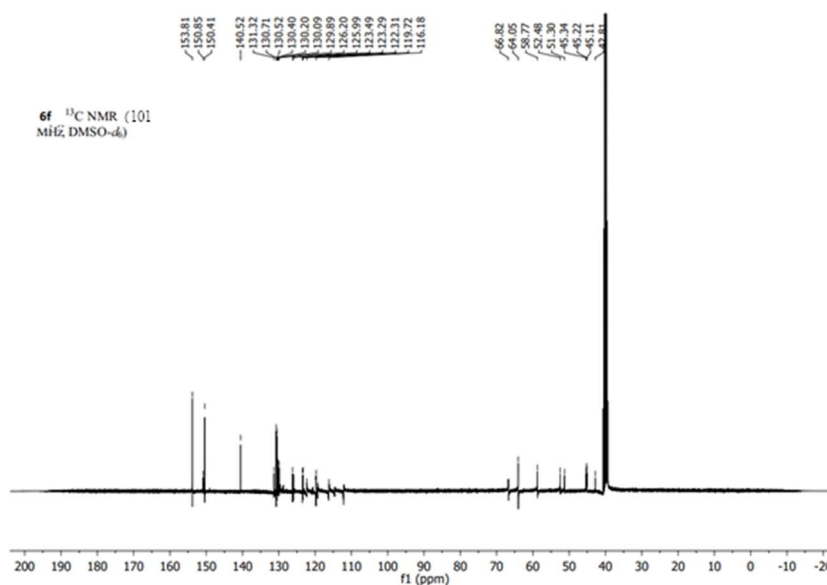


Figure S22. ^{13}C NMR Spectrum of the compound 6f.

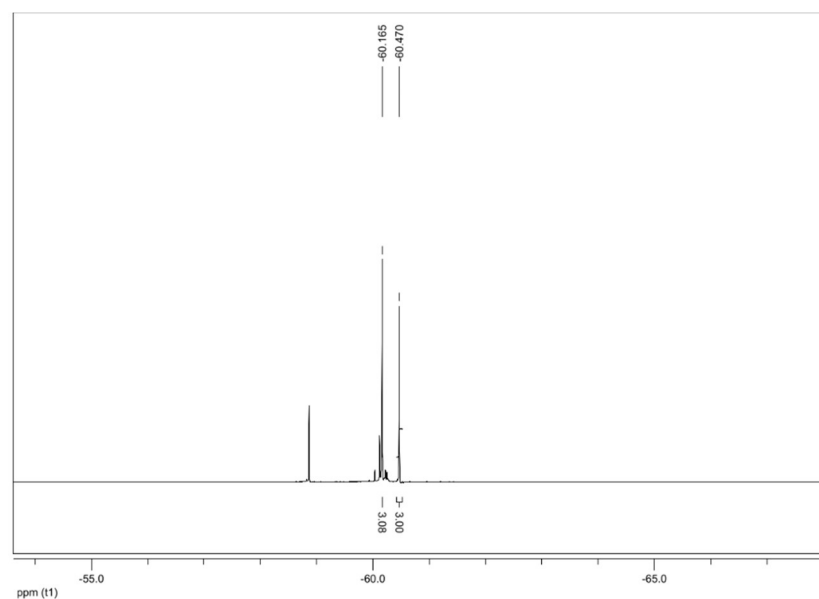


Figure S23. ^{19}F NMR Spectrum of the compound **6f**.

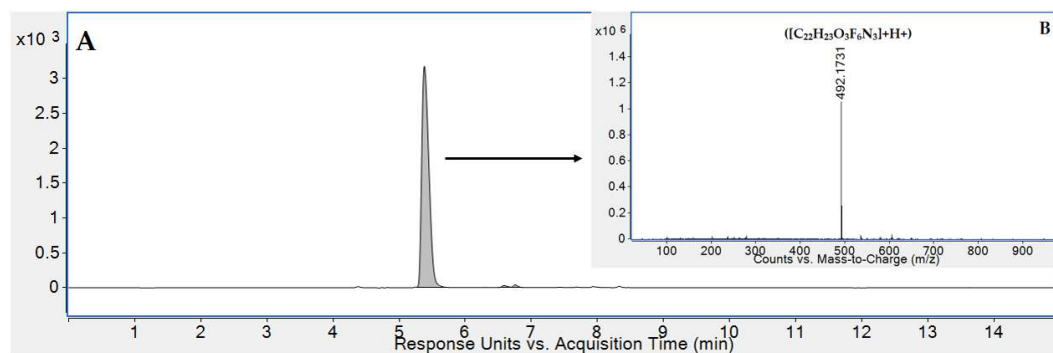


Figure S24. LC-UV-MS analysis of the compound **6f**. Panel A – purity profile (LC-UV –254 nm), panel B – HR-MS spectrum of the desired compound (the major peak from UV chromatogram).

C7. ^1H NMR, ^{13}C NMR, ^{19}F NMR and HPLC-UV/HR-MS (ESI) Spectra of 1-[2-Hydroxypropyl]-[(3-trifluoromethyl)phenyl]carbamoyloxy]-4-(4-diphenylmethyl)-piperazin-1-ium Chloride (**6g**)

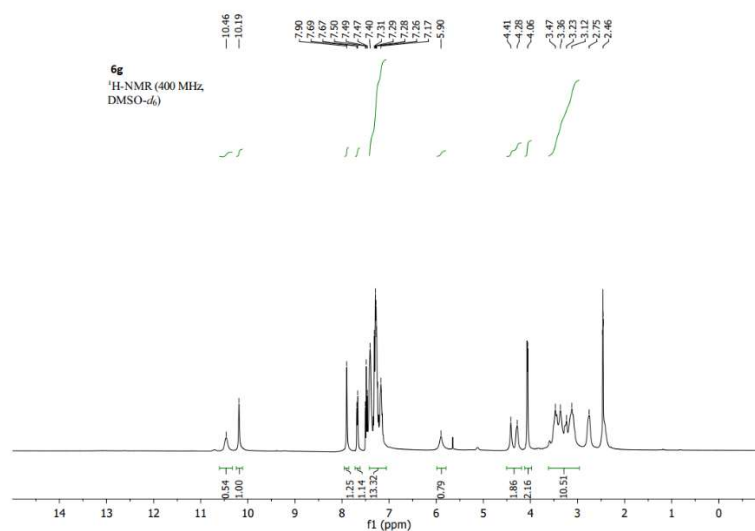


Figure S25. ^1H NMR Spectrum of the compound **6g**.

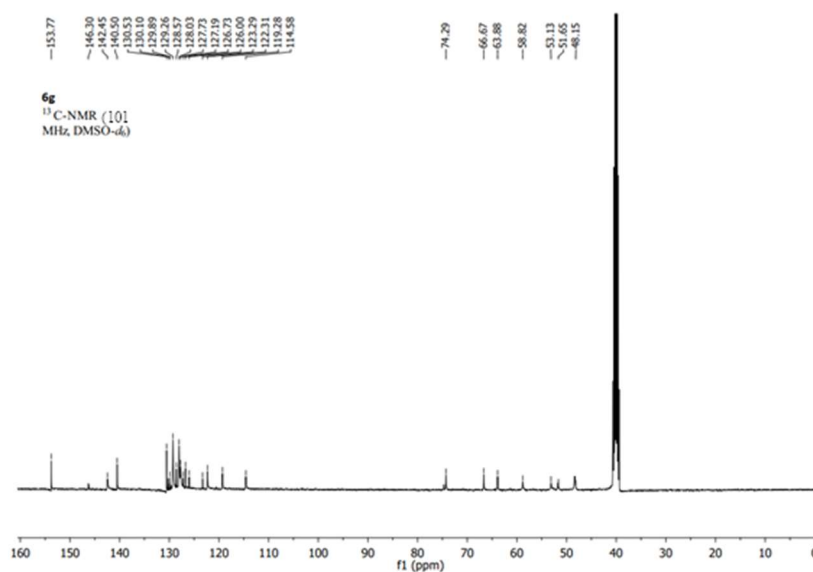


Figure S26. ^{13}C NMR Spectrum of the compound **6g**.

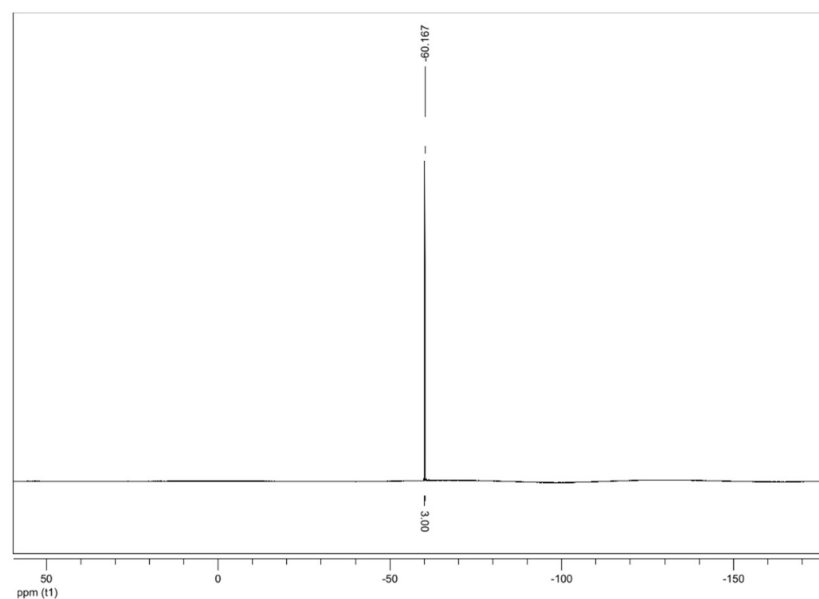


Figure S27. ^{19}F NMR Spectrum of the compound **6g**.

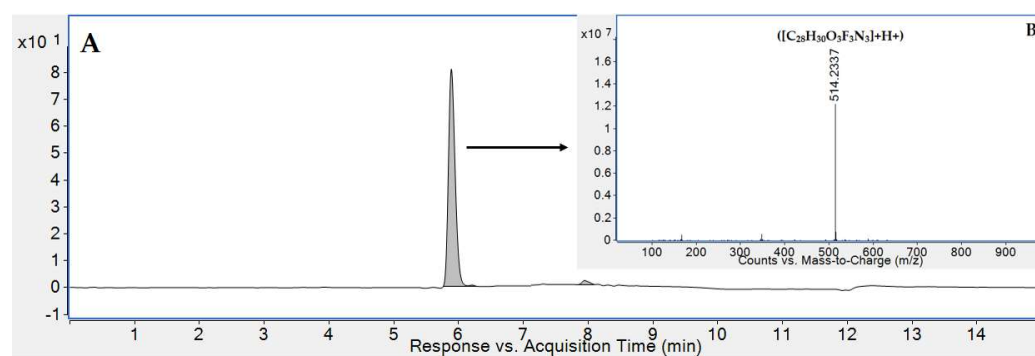


Figure S28. LC-UV-MS analysis of the compound **6g**. Panel A – purity profile (LC-UV –254 nm), panel B – HR-MS spectrum of the desired compound (the major peak from UV chromatogram).